

Deepening the Topology of the Translocator Protein Binding Site by Novel *N,N*-dialkyl-2-arylindol-3-ylglyoxylamides.

Elisabetta Barresi,^{‡,¥} Agostino Bruno,^{§,¥} Sabrina Taliani,^{‡,*} Sandro Cosconati,^{#,*} Eleonora Da Pozzo,[‡] Silvia Salerno,[‡] Francesca Simorini,[‡] Simona Daniele,[‡] Chiara Giacomelli,[‡] Anna Maria Marini,[‡] Concettina La Motta,[‡] Luciana Marinelli,[§] Barbara Cosimelli,[§] Ettore Novellino,[§] Giovanni Greco,[§] Federico Da Settimo,[‡] and Claudia Martini.[‡]

[‡]Dipartimento di Farmacia, Università di Pisa, Via Bonanno 6, 56126 Pisa, Italy

[§]Dipartimento di Farmacia, Università di Napoli “Federico II”, Via D. Montesano 49, 80131 Napoli, Italy

[#]DiSTABiF, Seconda Università di Napoli, Via Vivaldi 43, 81100 Caserta, Italy

Abstract

As a continuation of our studies on 2-phenylindol-3-ylglyoxylamides as potent and selective Translocator Protein (TSPO) ligands, two subsets of novel derivatives, featuring hydrophilic group (OH, NH₂, COOH) at the *para*-position of the pendant 2-phenyl ring (**8-16**) or different 2-aryl moieties, namely 3-thienyl, *p*-biphenyl, 2-naphthyl, (**23-35**), were synthesized and biologically evaluated, some of them showing *K_i* values in the subnanomolar range and the 2-naphthyl group performance being the best. The resulting SARs confirmed the key role played by interactions taking place between ligands and the lipophilic L1 pocket of the TSPO binding site. Docking simulations were performed on the most potent compound of the present series (**29**) exploiting the recently available 3D structures of TSPO bound to its standard ligand (PK11195). Our theoretical model was fully consistent with SARs of the newly investigated as well of the previously reported 2-phenylindol-3-ylglyoxylamide derivatives.

Introduction

The Translocator Protein (TSPO), first described as peripheral benzodiazepine receptor (PBR),^{1,2} is an 18 kDa protein mainly expressed in the outer mitochondrial membranes, where it interacts with a number of associated proteins including the voltage-dependent anion channel (VDAC, 32 kDa), the adenine nucleotide transporter (ANT, 30 kDa), the PBR associated protein-1 (PRAX-1, 220-250 kDa), the steroidogenesis regulatory protein (StAR, 37 kDa), and the TSPO and protein kinase A regulatory subunit RI α -associated protein (PAP7, 52 kDa).¹ Additional cellular locations of TSPO have been identified such as nucleus, lysosome, Golgi apparatus, peroxisomes, and plasma membrane.^{1,3} TSPO is an evolutionarily well-conserved and tryptophan-rich 169 amino acids protein organized into five transmembrane helices linked by hydrophobic loops, with a carboxy-terminal and a short amino-terminal tails located outside and inside the mitochondria, respectively.¹ Site-directed mutagenesis experiments,⁴ together with a recent NMR study,⁵ demonstrated that the portion of the receptor that recognizes the ligands is located at the bottom of the transmembrane bundle, also contacting the first cytoplasmatic loop.

TSPO is involved in numerous cellular processes related to the regulation of mitochondrial cholesterol translocation, porphyrin transport and heme synthesis, cellular proliferation and apoptosis, regulation of mitochondrial functions, immunomodulation and inflammation.^{1,4,6} This protein is ubiquitously expressed, with higher levels in tissues that produce steroids and that are mitochondrially enriched such as myocardium, skeletal muscle, and renal tissue;¹ other peripheral tissues, including liver and lung, express TSPO to a less extent.¹ In the central nervous system (CNS), TSPO is mainly located in glial cells, but it is also present in neurons.⁷ Such a distribution in the CNS may be related to the crucial role that TSPO plays in the regulation of cholesterol translocation from the outer to the inner mitochondrial membrane, where it is converted into pregnenolone, the precursor of all neurosteroids.⁸ A number of these endogenous molecules, such as pregnenolone and allopregnanolone, are able to rapidly inhibit neuron excitability as a result of a

positive allosteric modulation of type A receptors for GABA (GABA_A), the major inhibitory neurotransmitter in the brain.⁹

Altered expression of TSPO has been linked to multiple diseases, including anxiety, cancer, ischemia-reperfusion injury, brain injury, and neurodegenerative conditions such as Alzheimer's and Parkinson's diseases.¹⁰ In this view, TSPO ligands have potential as diagnostic tools for the state and progression of these related-diseases,^{10,11} as well as therapeutic antiproliferative and neuroprotective agents.¹²⁻¹⁴

Since identification of TSPO by means of the benzodiazepines diazepam and Ro5-4864 **1** (Chart 1),² structurally different classes of highly potent and selective ligands have been reported (Chart 1), including the isoquinolinecarboxamides, of which the 1-(2-chlorophenyl)-*N*-methyl-*N*-(1-methylpropyl)-1-isoquinolinecarboxamide (PK11195, **2**) is widely considered as a prototypical TSPO ligand,¹⁵ imidazopyridines (alpidem, **3**), indoleacetamides (FGIN-1-27, **4**),¹⁶ tetrahydrocarbazolecarboxamides (GE-180, **5**),¹⁷⁻¹⁹ and purineacetamides (AC-5216, **6**).²⁰⁻²⁴

In this context, we disclosed the *N,N*-dialkyl-2-phenylindol-3-ylglyoxylamides **7** as a class of potent and selective TSPO ligands (Chart 1), the majority of which showed *K_i* values in the nanomolar/subnanomolar range and were able to stimulate steroid biosynthesis in rat C6 glioma cells to an extent similar to or higher than that of classic TSPO ligands Ro5-4864, and PK11195.²⁵⁻²⁷ A large number of derivatives **7** was synthesized and biologically evaluated, featuring different combinations of R₁-R₅ substituents. The structure-affinity relationships (SARs) of these compounds were rationalized in light of a pharmacophore/topological model made up of three lipophilic pockets (L1, L3, and L4) and an H-bond donor group H1 (Chart 1).^{25,26,28} According to our model, the amide carbonyl oxygen of the oxalyl bridge engages an H-bond with the donor site H1; the two lipophilic substituents on the amide nitrogen, R₁, and R₂ interact through hydrophobic contacts with the L3 and/or L4 lipophilic pockets; the 2-phenyl moiety establishes a putative π -stacking interaction within the L1 pocket. The optimum binding affinity to TSPO in series **7** requires two lipophilic substituents on the amide nitrogen (R₁, R₂ = methyl, ethyl, *n*-propyl, *n*-butyl, *n*-pentyl, *n*-

hexyl, benzyl, etc.) to fit both in the L3 and L4 lipophilic pockets. Symmetrically ($R_1 = R_2$) and asymmetrically ($R_1 \neq R_2$) *N,N*-disubstituted indoles were investigated revealing that: (i) an aromatic moiety (R_1/R_2) is equivalent to an aliphatic one of similar size in taking hydrophobic contacts with the L3 or L4 lipophilic pocket; (ii) the L3 and L4 pockets are probably different in their dimensions as substitution pattern on the amide nitrogen with R_1 and R_2 of different sizes yielded high affinity derivatives. Moreover, the R_3 substituent has to feature electron-withdrawing properties to reinforce the putative π -stacking interaction within the L1 pocket, and R_4 has to be both electron-withdrawing and very small for optimal binding, a combination of properties only featured by the fluorine atom. Conversely, substitutions at position 7 of the indole nucleus (R_5) do not produce any affinity gain.^{25,26}

As stated above, TSPO may also represent a marker for related disease progression, so that the 2-phenylindolylglyoxylamide scaffold has been studied as a novel chemotype for the development of specific TSPO molecular probes. Novel reversible and irreversible fluorescent probes targeting TSPO were developed which featured the 7-nitrobenz-2-oxa-1,3-diazol-4-yl (NBD) group as a fluorophore.^{29,30} Furthermore, a new ¹¹C-radiolabeled probe from class **7**, the *N,N*-di-*n*-propyl-(*N*¹-methyl-2-(4'-nitrophenyl)indol-3-yl)glyoxylamide, was synthesized and evaluated with positron emission tomography in monkey, showing to enter brain and give a high proportion of TSPO-specific binding, auguring well for its future application in humans as biomarker of neuroinflammation.³¹

As a continuation of our studies on 2-phenylindol-3-ylglyoxylamides as potent and selective TSPO ligands, our attention has been now focused on the effects on binding affinity of different aryl moieties at the 2-position of the indole nucleus. The aim of our project was to probe the L1 lipophilic pocket and its surroundings to better define the whole topology of the TSPO binding site. For this purpose, a first subset of novel indole derivatives (**8-16**) were designed, featuring hydrophilic group (OH, NH₂, COOH) at the *para*-position of the pendant 2-phenyl ring. Actually, Trapani and colleagues reported that the introduction of polar and ionisable substituents at the *para*-

and *meta*-positions of the 2-phenyl ring of 2-phenylimidazopyridine TSPO ligands, yielded compounds showing very high affinity and selectivity for TSPO, with K_i values in the low nanomolar/subnanomolar range.³² To expand the SARs, derivatives **17-22** (Ar = *p*-CH₃O-C₆H₄ and *p*-CH₃OOC-C₆H₄, respectively), which are the intermediates in the synthesis of compounds **8-10** and **14-16** (see Scheme 1), were biologically evaluated. The second subset is represented by indoles **23-35**, which are functionalized at 2-position with aryl moieties different from the variously substituted phenyl ring, that is 3-thienyl (**23-25**), and the highly steric-demanding *p*-biphenyl (**26-28**) or 2-naphthyl (**29-35**) group.

All the novel indole derivatives **8-35** were biologically evaluated for their binding affinity to TSPO. Finally, a 3D model of the rTSPO was developed employing the newly published NMR model of mTSPO (PDB code: 2MGY),⁵ and docking studies were conducted using compound **29** as reference ligand, in order to rationalize the SARs within the 2-arylindol-3-ylglyoxylamide TSPO ligands described so far.

RESULTS AND DISCUSSION

Chemistry. The target *N,N*-dialkyl-2-(4-substituted-phenyl)indol-3-ylglyoxylamides **8-16**, *N,N*-dialkyl-2-(thien-3-yl)indol-3-ylglyoxylamides **23-25**, *N,N*-dialkyl-2-(*p*-biphenyl)indol-3-ylglyoxylamides **26-28**, and *N,N*-dialkyl-2-(naphth-2-yl)indol-3-ylglyoxylamides **29-35** were synthesized through the 2-arylindoles **36-38** and **42-44**, which were in turn simply obtained, with the exception of the commercially 2-(biphenyl-4-yl)indole **43** and 2-(naphth-2-yl)indole **44**, with a one-step Fischer indole synthesis by reacting phenylhydrazine hydrochloride and the appropriate acetyl derivative, Schemes 1 and 2. Under acid catalysis [excess of polyphosphoric acid (PPA)], the phenylhydrazone initially formed undergoes a number of isomerizations/rearrangements, and finally eliminates NH₃ to give the indole products.

Acylation of the appropriate 2-(4-substituted-phenyl)indole **36-38** with oxalyl chloride, in anhydrous diethyl ether, at room temperature, yielded the corresponding 2-(4-substituted-

phenyl)indolylglyoxylyl chlorides **39-41**, which were allowed to react with the appropriate dialkylamine, in the presence of triethylamine, in dry toluene solution, at room temperature, to give compounds **7d-f**, **17-22** (Scheme 1).

The indolylglyoxylamide derivatives featuring a OH group in R₃ (**8-10**) were achieved through a demethylation of the methoxy group of compounds **17-19** by treatment with BBr₃ in a nitrogen atmosphere (Scheme 1). At the end of the reaction, methanol was added to hydrolyze the excess of BBr₃, and crude compounds were recovered as a solid precipitated after evaporation under reduced pressure.

The *N,N*-dialkyl-[2-(4-nitrophenyl)indol-3-yl]glyoxylamide derivatives **7d-f** were catalytically hydrogenated over palladium to yield the corresponding 2-phenylindolylglyoxylamide analogues **11-13** bearing a NH₂ in *para*-position at the 2-phenyl ring (Scheme 1).

Finally, hydrolysis of the methyl ester group of compounds **20-22** with lithium hydroxide monohydrate, in a solution of methanol/water (3:1) gave the target compounds **14-16** (Scheme 1).

Scheme 2 outlined the general procedure for the synthesis of *N,N*-dialkyl-2-(aryl)indol-3-ylglyoxylamides **23-35**. The 2-arylindoles **42-44** were acylated with oxalyl chloride, in anhydrous diethyl ether, at room temperature, to obtain the corresponding indolylglyoxylyl chlorides **45-47**. The subsequent condensation with the appropriate amines, in the presence of triethylamine, in dry toluene solution, yielded the target derivatives **23-35**.

The reaction yields, the chemical physical constants and spectroscopic data of compounds **8-35** are listed in the Experimental Section.

The (2-arylindol-3-yl)glyoxylyl chlorides **39**, **41**, **45-47** have never been described before in the literature and were characterized as their corresponding ethyl ester derivatives (see Experimental Section).

Biological studies. The binding affinity of all the newly synthesized 2-arylindol-3-ylglyoxylamide derivatives **8-35** for the TSPO was determined by binding competition experiments against [³H]PK11195,^{25,26} carried out in rat kidney membrane homogenates (Tables 1 and 2). Because of

the well-established TSPO versus central benzodiazepine receptor (BzR) selectivity of *N,N*-dialkyl-2-phenylindol-3-ylglyoxylamides,^{25,26} a few randomly selected derivatives were evaluated for their BzR affinity by experiments against [³H]flumazenil in rat cerebral cortex membrane homogenates.^{25,26} The tested compounds showed no significant binding properties in this assay (inhibition percentages at 10 μ M concentration ranging from 0% to 23%, data not shown).

The TSPO binding affinities of compounds **8-22**, and **23-35**, expressed as K_i values, are listed in Tables 1, and 2, respectively, together with the K_i values of the standard TSPO ligands Ro5-4864, and PK11195 (Chart 1). The binding data of some of the previously investigated indole derivatives^{25,26} are included for comparison at the bottom of Table 1 (**7a-f**) and Table 2 (**7a-c, g-j**).

In the **8-16** series, the amide nitrogen is symmetrically disubstituted ($R_1 = R_2$, Table 1) with *n*-propyl, *n*-butyl, and *n*-hexyl chains and the 2-phenyl moiety is decorated by small hydrophilic groups inserted at the *para*-position ($R_3 = \text{OH}, \text{NH}_2, \text{COOH}$, Table 1); derivatives **17-22** ($R_3 = \text{OCH}_3, \text{COOCH}_3$, Table 1), which are the intermediates in the synthesis of compounds **8-10** and **14-16**, respectively (see Scheme 1), were also biologically evaluated to expand the SARs.

In general, the introduction of a hydrophilic group at the *para*-position of the 2-phenyl ring (OH, NH₂, COOH) did not determine any significant improvement of the affinity, suggesting that the interaction at the level of the L1 pocket is mostly lipophilic (Table 1). In particular, the insertion of an OH group at the *para*-position of the 2-phenyl ring is tolerated for affinity (**8** K_i 16.1 nM, **9** K_i 25.7 nM, **10** K_i 6.3 nM, vs **7a** K_i 12.2 nM, **7b** K_i 7.5 nM, **7c** K_i 1.4 nM, respectively). Conversely, a decrease of the binding affinity is observed introducing a NH₂ (**11** K_i 44.4 nM, **12** K_i 133 nM, **13** K_i 4.2 nM, vs **7a** K_i 12.2 nM, **7b** K_i 7.5 nM, **7c** K_i 1.4 nM, respectively) or, to a major extent, a COOH group (**14** K_i 343 nM, **15** K_i 406 nM, **16** K_i 184 nM vs **7a** K_i 12.2 nM, **7b** K_i 7.5 nM, **7c** K_i 1.4 nM, respectively, Table 1). In addition, in all the subsets, compounds bearing *n*-hexyl chains on the symmetrically disubstituted amide nitrogen are more potent than the others. A different trend is observed for derivatives **17-19** and **20-22**, featuring a *p*-methoxy and *p*-methoxycarbonyl substituent, respectively, that show, with the exception of compound **18** (K_i 20.3 nM), appreciable

and comparable affinity (K_i values in the low nanomolar range), whatever is the length of the side alkyl chains, Table 1.

The data listed in Table 2 evidence that the replacement of the 2-phenyl group with a thien-3-yl (**23-25**), a *p*-biphenyl (**26-28**), or a naphth-2-yl (**29-35**) moiety produces, with few exceptions, superior affinity TSPO ligands, with K_i values in the subnanomolar range. As the presence of a naphthyl group seemed to be particularly favourable for affinity, this subset was further investigated by the synthesis of a number of asymmetrically *N,N*-disubstituted indoles (**32-35**, Table 2), to more deeply probe the L3 and L4 lipophilic pockets of the TSPO binding site (R_1 = methyl, ethyl; R_2 = *n*-butyl, *n*-pentyl, benzyl). Interestingly, within the subset of the 2-(naphth-2-yl)-substituted derivatives **29-35**, all compounds showed almost identical K_i values in the subnanomolar range, ranging from 0.30 nM to 0.56 nM (Table 2). Thus, the nature of the groups bound to the amide nitrogen does not significantly influence the binding of ligands **29-35** at TSPO. These data suggest a key role played by the lipophilic interaction at the level of the L_1 pocket that, reaching its optimum with a naphthyl group, makes less significant the contribution to the binding of the remaining lipophilic interactions established by the ligand within the receptor binding site.

Due to the well-established steroidogenic effect of derivatives from the 2-phenylindol-3-ylglyoxylamide class,^{25,26} compound **29** was selected and routinely evaluated for its ability to stimulate pregnenolone formation from rat C6 glioma cells,^{25,26} showing an increase percentage in pregnenolone production *vs* control similar to that of the reference standard PK11195^{25,26} (see Supplementary Information for Method details).

Computational Studies: rTSPO model construction and docking calculations. A survey in the available literature demonstrates that, to date, several X-ray^{33,34} and solution⁵ (NMR) structures were deposited in the Protein Data Bank (PDB).³⁵ Among them, we decided to choose the solution one (mTSPO) as a template for the construction of our rTSPO model, given the higher sequence identity shared by the two proteins (95%). Therefore, several 3D models of the rTSPO were generated using the newly published NMR model of mTSPO (PDB code: 2MGY),⁵ by applying the

following protocol: (i) 20 NMR snapshots are available in the structure of the mTSPO and we used each of them as a template for the construction of the rTSPO; (ii) for each template, 20 models were generated making a total of 400 rTSPO models, grouped in 20 groups (one for each NMR snapshot); (iii) then, the best rTSPO models in each group were selected (i.e. the models giving the highest score according to the modeller native scoring function and featuring the best Ramachandran plots) for a total of 20 rTSPO structures. The selected 20 rTSPO models were refined through the protein preparation protocol available in Maestro9.8.³⁶

Comparison between the rTSPO model (see docking studies) and its corresponding mTSPO NMR snapshot template is depicted in Supplementary Figure S1 (SI), with the corresponding Ramachandran plots.

Docking was performed using Glide tool of Maestro 9.8³⁶ on the 20 selected mTSPO structures. To set up the docking studies the following considerations were made: (i) the stoichiometry of the protein-ligand interaction is 1:1;⁵ (ii) the indolyglyoxylamide derivatives are competing for the same PK11195 binding site.^{25-27,29} On the basis of these observations, the docking studies were conducted on the monomeric rTSPO, and using compound **29** as reference ligand (i.e. the one endowed with the best binding properties). Among the 20 **29**/rTSPO generated complexes, we considered only those in which: i) the ligand was occupying the same PK11195 binding regions (17 complexes), ii) there was agreement with the SARs reported by us in literature^{25-27,29,37} and in this work (2 complexes). Of these latter complexes, we considered the one having the highest glide score (1 complex) (Supplementary Figure S2, SI).

The binding mode and the SARs of the indolyglyoxylamide derivatives. Glide software³⁶ predicts **29** to fairly recapitulate the experimental TSPO/ PK11195 interactions (see Supplementary Figure S3, SI), so that the ligand is nicely adapted in the mainly hydrophobic binding pocket of rTSPO (see Figure 1a). In the proposed binding mode of **29** to TSPO, the naphthyl moiety is placed inside a roomy aromatic cage (herein referred to as L1 pocket), establishing hydrophobic interaction with V110, W95, W107, L114, W143, F146 and L150 residues. This is in agreement with our

previous works^{21,22,24 25-27} showing that, among the indolylglyoxylamides, *p*-substitution of the phenyl ring at position 2 of the indole ring results in higher affinity with respect to the unsubstituted phenyl moiety (i.e. **7a** vs **7d**). Interestingly, given the aromatic/hydrophobic nature of the L1 region, it is not surprising that R₃ polar and/or electron-donating groups are generally less tolerated than hydrophobic and/or electron-withdrawing ones. In particular, in the proposed binding mode (Figure 1a-c), the aromatic ring at position 2 of the indole ring establishes a parallel displaced π - π interaction with W107, thus explaining the general correlation between the R₃ electron-withdrawing effect and the affinity for rTSPO observed for the *N,N*-dipropyl (**7d** > **20** > **17** > **7a** > **8** > **11** > **14**) and for the *N,N*-dibutyl (**7e** > **21** > **7b** > **18** > **9** > **12** > **15**) series, but less evident for the *N,N*-dihexyl one (**7f** > **7c** > **22** > **13** > **19** > **10** > **16**) (See Supplementary Figure S4, SI, for a qualitative correlation). This observation highlights that a cooperative effect between the nature of the substituents on the *N,N*-alkyl branches and the electronic nature of the substituents in R₃ exists, and in turn a proper balance is required. Indeed, in the case of the *N,N*-dihexyl derivatives, the hydrophobic nature of the *N,N*-alkyl branches predominates over the electronic effects of the R₃ substituents.

The extension and the chemical nature of the cleft lodging in the aforementioned group (Figure 1a-d) would also explain why substitution with a biphenyl (**26**) results in comparably high affinities, while the presence of the smaller phenyl/thienyl groups results in lower binding (**29** = **26** > **23** > **7a**).

According to the present binding mode (Figure 1a) the *N*-propyl branch in the *cisoid* configuration protrudes toward the membrane environment, while the second *N*-propyl branch establishes hydrophobic interactions with V26, W107, and L150.

The proposed theoretical model (Figure 1a) is also in agreement with our previous works where fluorescent probes were developed.²⁹ In particular, we derivatized our 2-phenylindol-3-ylglyoxylamides with a 7-nitrobenz-2-oxa-1,3-diazol-4-yl (NBD) group that is well-known for displaying low quantum yields in water, while becoming highly fluorescent in more lipophilic

environments, such as membranes or hydrophobic receptor pockets.³⁰ Indeed, according to our model, the attached NBD linker would be hosted outside the receptor in the membrane environment, thus explaining why our previously published TSPO NBD-labelled fluorescent probes²⁹ are so efficient in staining rat and human glioma cells.

The position of the *N,N*-disubstituted branches would also explain why bulkier substituents on the ligand amide moiety do not significantly affect the activity for the naphthyl derivatives (**29** vs **30-35**). Interestingly, the amide branches accommodates in a similar region with respect to the amide branches of the PK11195 (Supplementary Figure S3, SI), and we already demonstrated in our previous works that bulkier substituents are well tolerated in this region.^{5,21,22,24,26,27,35} Differently from the naphthyl series (**29-35**), the biphenyl one seems to be affected by the presence of bulkier substituents on the amide branch of the glyoxylamide moiety (**26** vs **27, 28**). This effect can be explained by the different bulkiness and shape of the biphenyl moiety with respect to the naphthyl one (Figure 1b-d and Supplementary Figure S5, SI), which in turn does not tolerate bulkier substituents on the amide group.

Furthermore, on the basis of the proposed binding mode (Figure 1a), the hydrophobic residues A23, W53, L49, and W143 surround the indole ring of **29**. This agrees with our previous works showing that substitutions on position 5 and 7 of the indole ring are tolerated.²⁵⁻²⁷ Finally, in our previous works, based on pharmacophoric models, it was suggested that the distal carbonyl oxygen of the oxalyl bridge engages an H-bond with the donor site H1 of the pharmacophore/topological model (Chart 1), in the TSPO binding site.²⁵⁻²⁷ On the contrary, the present binding mode lacks any polar interaction between the glyoxylamide branch and the receptor binding site (Figure 1a). In this regard, it can be argued that the presence of the amide/glyoxylamide groups in TSPO binders, rather than engaging specific interactions with the receptor, has a role in constraining the flexibility of the ligand branch so as to adopt the bioactive conformation. We cannot rule out the presence of water molecules inside the TSPO binding pocket that mediate polar interactions between the amide/glyoxylamide and the protein binding site. The same interaction (H-bond with the H1 site)

was also postulated in a previous paper for the PK11195/TSPO pharmacophore/topological model³⁸ and was not lately verified by the NMR experimental structure.⁵

CONCLUSIONS

Novel 2-arylindol-3-ylglyoxylamides were synthesized and biologically evaluated to clarify the effect of different aryl moieties at the 2-position of the indole nucleus on modulation of affinity to TSPO, and thus to probe the L1 lipophilic pocket and its surroundings.

Within the first subset of novel indole derivatives (**8-16**), the introduction of a hydrophilic group at the *para*-position of the 2-phenyl ring (OH, NH₂, COOH) does not determine any significant improvement of the affinity; conversely, the replacement of the 2-phenyl group with thien-3-yl (**23-25**), *p*-biphenyl (**26-28**), or naphth-2-yl (**29-35**) moiety produces, with few exceptions, superior affinity TSPO ligands, with K_i values in the subnanomolar range. Of note, within the subseries of the 2-(naphth-2-yl)-substituted derivatives **29-35**, all compounds showed almost identical K_i subnanomolar values, independently from the nature of the groups bound to the amide nitrogen. Taken together, the SARs suggest a key role of the lipophilic interaction at the level of the L1 pocket that, when reaches its optimum with a naphthyl group, makes less significant all the other lipophilic interactions of the molecule within the receptor protein.

A 3D model of the rTSPO was developed employing the newly published NMR model of mTSPO (PDB code: 2MGY).⁵ Docking studies were conducted using compound **29** as reference ligand, and the proposed binding mode highlighted the cooperative effects between the nature of the substituents on the *N,N*-alkyl branches and the electronic features of the moiety at indole 2-position, rationalizing the SARs within the 2-arylindol-3-ylglyoxylamide TSPO ligands described so far.

EXPERIMENTAL SECTION

Chemistry. Evaporation was performed in vacuo (rotary evaporator). Analytical TLC was carried out on Merck 0.2 mm precoated silica gel aluminum sheets (60 F-254). Silica gel 60 (230-400

mesh) was used for column chromatography. Melting points were determined using a Reichert Köfler hot-stage apparatus and are uncorrected. Routine nuclear magnetic resonance spectra were recorded in DMSO-*d*₆ solution on a Varian Gemini 200 spectrometer operating at 200 MHz. The NMR spectra of tertiary amides show the presence of two different conformational isomers (ratio about 1:1) in equilibrium (see ref. n° 26,37 for details). Elemental analyses were performed by our analytical laboratory and agreed with theoretical values to within (0.4%).

2-(*p*-Biphenyl-4-yl)indole **43** and 2-(naphth-2-yl)indole **44** are commercially available. 2-(4-Methoxyphenyl)indole **36**,³⁹ 2-(4-nitrophenyl)indole **37**,²⁶ 2-(3-thienyl)-1*H*-indole **42**,⁴⁰ [2-(4-nitrophenyl)indol-3-yl]glyoxylyl chloride **40**,²⁶ *N,N*-di-*n*-propyl-[2-(4-nitrophenyl)indol-3-yl]glyoxylamide **7d**,²⁶ *N,N*-di-*n*-butyl-[2-(4-nitrophenyl)indol-3-yl]glyoxylamide **7e**,²⁶ *N,N*-di-*n*-hexyl-[2-(4-nitrophenyl)indol-3-yl]glyoxylamide **7f**,²⁶ were prepared in accordance with reported procedures.

Methyl-4-(1*H*-indol-2-yl)benzoate 38. 1 g of polyphosphoric acid (PPA) was added to a mixture of phenylhydrazine hydrochloride (0.541 g, 5.0 mmol) and methyl 4-acetylbenzoate (0.891 g, 5.0 mmol). The reaction was maintained at 60 °C for 4 h and then poured into ice (ca 100 g). The precipitated solid was collected by filtration and purified by recrystallization from toluene (30 mL). Yield: 78%; mp 204-207 °C, lit. ref. n° 41 mp 206.3-207.5 °C.

General procedure for the synthesis of [2-(4-substituted-phenyl)indol-3-yl]glyoxylyl chloride derivatives 39, 41, and (2-arylindol-3-yl)glyoxylyl chloride derivatives 45-47. Oxalyl chloride (8.0 mmol) was added dropwise at 0 °C to a well-stirred mixture of the appropriate indole **36**, **38**, **42-44** (4.0 mmol) in freshly distilled diethyl ether (10 mL). The mixture was maintained at room temperature for 2-24 h (TLC analysis). The precipitate formed was collected and washed with portions of diethyl ether (20 mL) to give the desired glyoxylyl chlorides, which were dried over P₂O₅ in vacuo and directly used in the subsequent reaction. All glyoxylyl chloride derivatives, were characterized by conversion into their corresponding ethyl esters.

[2-(4-Methoxyphenyl)indol-3-yl]glyoxylyl chloride (39). Yield: 72%

Ethyl [2-(4-methoxyphenyl)-1H-indol-3-yl](oxo)acetate 39a. Yield: 70%; mp 194-196 °C. ¹H-NMR (DMSO-*d*₆, ppm): 0.99 (t, *J* = 7.2 Hz, 3H, CH₂CH₃); 3.68 (q, *J* = 7.2 Hz, 2H, CH₂CH₃); 3.85 (s, 3H, OCH₃); 7.12 (d, *J* = 6.8 Hz, 2H, 3'-H, 5'-H); 7.26-7.33 (m, 2H, Ar-H); 7.49-7.52 (m, 3H, Ar-H); 8.12-8.15 (m, 1H, 4-H); 12.52 (bs, 1H, NH, exch. with D₂O). Anal. Calcd for C₁₉H₁₇NO₄: C, 70.58; H, 5.30; N, 4.33. Found: C, 70.45; H, 5.17; N, 4.27.

Methyl 4-{3-[chloro(oxo)acetyl]-1H-indol-2-yl} benzoate (41). Yield: 80%

Methyl 4-{3-[ethoxy(oxo)acetyl]-1H-indol-2-yl}benzoate 41a. Yield: 70%; mp 152-154 °C. ¹H-NMR (DMSO-*d*₆, ppm): 0.97 (t, *J* = 7.2 Hz, 3H, CH₂CH₃); 3.63 (q, *J* = 7.2 Hz, 2H, CH₂CH₃); 3.92 (s, 3H, OCH₃); 7.32-7.36 (m, 2H, Ar-H); 7.54-7.57 (m, 1H, Ar-H); 7.74 (d, *J* = 8.4 Hz, 2H, 2'-H, 6'-H); 8.11-8.16 (m, 3H, Ar-H); 12.80 (bs, 1H, NH, exch. with D₂O). Anal. Calcd for C₂₀H₁₇NO₅: C, 68.37; H, 4.88; N, 3.99. Found: C, 68.51; H, 4.71; N, 4.05.

Oxo[2-(3-thienyl)-1H-indol-3-yl]acetyl chloride (45). Yield: 65%

Ethyl oxo[2-(3-thienyl)-1H-indol-3-yl]acetate 45a. Yield: 72%; mp 168-170 °C. ¹H-NMR (DMSO-*d*₆, ppm): 1.06 (t, *J* = 7.2 Hz, 3H, CH₂CH₃); 3.82 (q, *J* = 7.2 Hz, 2H, CH₂CH₃); 7.28-7.33 (m, 2H, Ar-H); 7.37-7.40 (m, 1H, Ar-H); 7.48-7.51 (m, 1H, Ar-H); 7.77-7.79 (m, 1H, Ar-H); 7.93-7.94 (m, 1H, Ar-H); 8.07-8.09 (m, 1H, 4-H); 12.59 (bs, 1H, NH, exch. with D₂O). Anal. Calcd for C₁₆H₁₃NO₃S: C, 64.20; H, 4.38; N, 4.68. Found: C, 64.08; H, 4.47; N, 4.75.

(2-Biphenyl-4-yl-1H-indol-3-yl)(oxo)acetyl chloride (46). Yield: 80%

Ethyl (2-biphenyl-4-yl-1H-indol-3-yl)(oxo)acetate 46a. Yield: 90%; mp 145-147 °C. ¹H-NMR (DMSO-*d*₆, ppm): 0.98 (t, *J* = 7.2 Hz, 3H, CH₂CH₃); 3.67 (q, *J* = 7.2 Hz, 2H, CH₂CH₃); 7.31-7.36 (m, 2H, Ar-H); 7.42-7.46 (m, 1H, Ar-H); 7.52-7.55 (m, 3H, Ar-H); 7.67 (d, *J* = 8.2 Hz, 2H, 3'-H, 5'-H); 7.76-7.78 (m, 2H, Ar-H); 7.88 (d, *J* = 8.2 Hz, 2H, 2'-H, 6'-H); 8.16-8.18 (m, 1H, 4-H); 12.70 (bs, 1H, NH, exch. with D₂O). Anal. Calcd for C₂₄H₁₉NO₃: C, 78.03; H, 5.18; N, 3.79. Found: C, 78.19; H, 5.33; N, 3.61.

[2-(2-Naphthyl)-1H-indol-3-yl](oxo)acetyl chloride (47). Yield: 82%

Ethyl [2-(2-naphthyl)-1H-indol-3-yl](oxo)acetate 47a. Yield: 79%; mp 143-145 °C. ¹H-NMR (DMSO-*d*₆, ppm): 0.79 (t, *J* = 7.2 Hz, 3H, CH₂CH₃); 3.34 (q, *J* = 7.2 Hz, 2H, CH₂CH₃); 7.32-7.38

(m, 2H, Ar-H); 7.56-7.58 (m, 1H, Ar-H); 7.64-7.66 (m, 2H, Ar-H); 7.70-7.72 (m, 1H, Ar-H); 8.04-8.06 (m, 2H, Ar-H); 8.09-8.14 (m, 2H, Ar-H); 8.19-8.21 (m, 1H, 4-H); 12.76 (bs, 1H, NH, exch. with D₂O). Anal. Calcd for C₂₂H₁₇NO₃: C, 76.95; H, 4.99; N, 4.08. Found: C, 77.10; H, 4.83; N, 4.17.

General procedure for the synthesis of *N,N*-dialkyl-[2-(4-substituted-phenyl)indol-3-yl]glyoxylamide derivatives 17-22, and *N,N*-dialkyl-[(2-arylindol)-3-yl]glyoxylamide derivatives 23-35. A solution of the appropriate amine (2.0 mmol) in 5 mL of dry toluene was added dropwise to a stirred suspension, cooled at 0 °C, of the glyoxylyl chlorides **39-41**, **45-47** (2.0 mmol) in 50 mL of the same solvent, followed by the addition of triethylamine (2.0 mmol). The reaction mixture was left under stirring for 2-24 h at room temperature (TLC analysis), and then filtered. The collected precipitate was triturated with a 5% NaHCO₃ aqueous solution (10 mL), washed with water (10 mL), and collected again to give a first portion of crude product. The toluene was removed under reduced pressure, and the oily residue dissolved with CHCl₃ (20-30 mL). The organic solution was washed with diluted HCl (10 mL), a 5% NaHCO₃ aqueous solution (10 mL) and water (10 mL), dried (MgSO₄), and evaporated to dryness to yield an additional amount of crude products, which were finally purified by flash chromatography (CHCl₃ as eluent).

2-[2-(4-Methoxyphenyl)-1*H*-indol-3-yl]-2-oxo-*N,N*-dipropylacetamide (17). Yield: 72%; mp 121-123 °C. ¹H-NMR (DMSO-*d*₆, ppm, mixture of conformational isomers): 0.68, 0.76 (2t, *J* = 7.2 Hz, 6H, 2(CH₂)₂CH₃); 1.21-1.26, 1.39-1.47 (2m, 4H, 2CH₂CH₂CH₃); 2.93-3.06 (m, 4H, 2NCH₂); 3.83 (s, 3H, OCH₃); 7.06 (d, *J* = 8.8 Hz, 2H, 3'-H, 5'-H); 7.18-7.30 (m, 2H, Ar-H); 7.44-7.56 (m, 3H, Ar-H); 7.99-8.04 (m, 1H, 4-H); 12.34 (bs, 1H, NH, exch. with D₂O). ¹³C-NMR (DMSO-*d*₆, ppm, mixture of conformational isomers): 11.38; 11.76; 20.55; 21.71; 46.03; 49.76; 55.82; 109.84; 112.39; 113.94; 121.20; 122.71; 123.44; 123.66; 127.35; 131.81; 136.14; 147.75; 160.90; 168.18; 187.62. Anal. Calcd for C₂₃H₂₆N₂O₃: C, 72.99; H, 6.92; N, 7.40. Found: C, 73.12; H, 6.80; N, 7.33.

***N,N*-Dibutyl-2-[2-(4-methoxyphenyl)-1*H*-indol-3-yl]-2-oxoacetamide (18).** Yield: 75%; mp 119-121 °C. ¹H-NMR (DMSO-*d*₆, ppm, mixture of conformational isomers): 0.72, 0.84 (2t, *J* = 7.0 Hz,

6H, 2(CH₂)₃CH₃); 1.02-1.13 (m, 6H, Aliph-H); 1.35-1.43 (m, 2H, Aliph-H); 2.98-3.07 (m, 4H, 2NCH₂); 3.83 (s, 3H, OCH₃); 7.06 (d, *J* = 8.8 Hz, 2H, 3'-H, 5'-H); 7.20-7.28 (m, 2H, Ar-H); 7.44-7.55 (m, 3H, Ar-H); 8.03-8.06 (m, 1H, 4-H); 12.53 (bs, 1H, NH, exch. with D₂O). ¹³C-NMR (DMSO-*d*₆, ppm, mixture of conformational isomers): 13.89; 14.11; 19.70; 20.23; 29.28; 30.40; 43.89; 47.55; 55.77; 109.87; 112.37; 113.91; 121.24; 122.70; 123.38; 123.67; 127.38; 131.86; 136.17; 147.79; 160.88; 168.00; 187.70. Anal. Calcd for C₂₅H₃₀N₂O₃: C, 73.86; H, 7.44; N, 6.89. Found: C, 73.72 ; H, 7.51; N, 6.99.

***N,N*-Dihexyl-2-[2-(4-methoxyphenyl)-1*H*-indol-3-yl]-2-oxoacetamide (19).** Yield: 65%; oil. ¹H-NMR (DMSO-*d*₆, ppm, mixture of conformational isomers): 0.73-1.36 (m, 22H, Aliph-H); 2.98-3.05 (m, 4H, 2NCH₂); 3.81 (s, 3H, OCH₃); 7.05 (d, *J* = 6.8 Hz, 2H, 3'-H, 5'-H); 7.20-7.25 (m, 2H, Ar-H); 7.43-7.54 (m, 3H, Ar-H); 8.01-8.04 (m, 1H, 4-H); 12.33 (bs, 1H, NH, exch. with D₂O). ¹³C-NMR (DMSO-*d*₆, ppm, mixture of conformational isomers): 14.20; 14.36; 22.26; 22.47; 26.02; 26.64; 27.09; 28.19; 31.08; 31.46; 43.57; 47.79; 55.77; 109.87; 112.38; 113.90; 121.26; 121.65; 122.32; 123.35; 127.35; 131.87; 136.19; 148.12; 159.34; 168.00; 187.91. Anal. Calcd for C₂₉H₃₈N₂O₃: C, 75.29; H, 8.28; N, 6.06. Found: C, 75.13; H, 8.21; N, 6.00.

Methyl 4-{3-[(dipropylamino)(oxo)acetyl]-1*H*-indol-2-yl}benzoate (20). Yield: 65%; mp 139-141 °C; ¹H-NMR (DMSO-*d*₆, ppm, mixture of conformational isomers): 0.66-0.77 (m, 6H, 2(CH₂)₂CH₃); 1.20-1.27, 1.45-1.49 (2m, 4H, 2CH₂CH₂CH₃); 2.93-3.10 (m, 4H, 2NCH₂); 3.92 (s, 3H, OCH₃); 7.27-7.31 (m, 2H, Ar-H); 7.50-7.54 (m, 1H, Ar-H); 7.74 (d, *J* = 8.0 Hz, 2H, 2'-H, 6'-H); 8.02-8.09 (m, 3H, 4-H); 12.64 (bs, 1H, NH, exch. with D₂O). ¹³C-NMR (DMSO-*d*₆, ppm, mixture of conformational isomers): 11.38; 11.71; 20.46; 21.77; 46.03; 49.77; 52.83; 110.49; 112.79; 121.27; 123.02; 124.10; 127.13; 129.10; 130.74; 130.82; 136.12; 136.51; 146.10; 166.37; 167.95; 187.37. Anal. Calcd for C₂₄H₂₆N₂O₄: C, 70.92; H, 6.45; N, 6.89. Found: C, 7.79; H, 6.53; N, 6.95.

Methyl 4-{3-[(dibutylamino)(oxo)acetyl]-1*H*-indol-2-yl}benzoate (21). Yield: 71%; mp 119-121 °C; ¹H-NMR (DMSO-*d*₆, ppm, mixture of conformational isomers): 0.69-0.80 (m, 6H, 2(CH₂)₃CH₃); 1.00-1.15 (m, 4H, 2(CH₂)₂CH₂CH₃); 1.25-1.41 (m, 4H, 2CH₂CH₂CH₂CH₃); 2.95-

3.09 (m, 4H, 2NCH₂); 3.89 (s, 3H, OCH₃); 7.25-7.30 (m, 2H, Ar-H); 7.48-7.52 (m, 1H, Ar-H); 7.72 (d, *J* = 8.0 Hz, 2H, 2'-H, 6'-H); 8.04-8.09 (m, 3H, 4-H); 12.59 (bs, 1H, NH, exch. with D₂O). ¹³C-NMR (DMSO-*d*₆, ppm, mixture of conformational isomers): 13.90; 14.01; 19.70; 20.16; 29.12; 30.41; 43.93; 47.55; 52.78; 110.63; 112.70; 121.42; 123.06; 124.17; 127.17; 129.17; 130.81; 130.90; 136.01; 136.42; 146.08; 166.32; 167.69; 187.56. Anal. Calcd for C₂₆H₃₀N₂O₄: C, 71.87; H, 6.96; N, 6.45. Found: C, 71.72; H, 6.89; N, 6.54.

Methyl 4-{3-[(dihexylamino)(oxo)acetyl]-1*H*-indol-2-yl}benzoate (22). Yield: 65%; oil. ¹H-NMR (DMSO-*d*₆, ppm, mixture of conformational isomers): 0.66-1.46 (m, 22H, Aliph-H); 2.85-2.97 (m, 4H, 2NCH₂); 3.81 (s, 3H, OCH₃); 7.18-7.21 (m, 2H, Ar-H); 7.39-7.42 (m, 1H); 7.64 (d, *J* = 7.8 Hz, 2H, 2'-H, 6'-H); 7.96-8.00 (m, 3H, Ar-H); 12.53 (bs, 1H, NH, exch. with D₂O). ¹³C-NMR (DMSO-*d*₆, ppm, mixture of conformational isomers): 14.19; 14.33; 22.28; 22.47; 26.03; 26.60; 26.87; 28.14; 31.09; 31.45; 44.18; 47.76; 52.76; 110.61; 112.67; 121.43; 123.04; 124.17; 127.14; 129.16; 130.79; 130.91; 135.96; 136.39; 145.98; 166.29; 167.67; 187.61. Anal. Calcd for C₃₀H₃₈N₂O₄: C, 73.44; H, 7.81; N, 5.71. Found: C, 73.56; H, 7.72; N, 5.65.

2-Oxo-*N,N*-dipropyl-2-[2-(3-thienyl)-1*H*-indol-3-yl]acetamide (23). Yield: 78%; mp 69-71 °C. ¹H-NMR (DMSO-*d*₆, ppm, mixture of conformational isomers): 0.65, 0.71 (2t, *J* = 7.2 Hz, 6H, 2(CH₂)₂CH₃); 1.30-1.50 (m, 4H, 2CH₂CH₂CH₃); 3.00-3.14 (m, 4H, 2NCH₂); 7.21-7.27 (m, 2H, Ar-H); 7.46-7.50 (m, 2H, Ar-H); 7.69-7.73 (m, 1H, Ar-H); 7.89-7.93 (m, 1H, 4-H); 8.13 (s, 1H, 2'-H); 12.45 (bs, 1H, NH, exch. with D₂O). ¹³C-NMR (DMSO-*d*₆, ppm, mixture of conformational isomers): 11.36; 11.81; 20.64; 21.73; 46.09; 49.72; 109.87; 112.48; 120.92; 122.75; 123.85; 126.53; 127.05; 128.74; 129.23; 131.42; 136.05; 142.02; 168.49; 187.32. Anal. Calcd for C₂₀H₂₂N₂O₂S: C, 67.77; H, 6.26; N, 7.90. Found: C, 67.91; H, 6.19; N, 7.95.

***N,N*-Dibutyl-2-oxo-2-[2-(3-thienyl)-1*H*-indol-3-yl]acetamide (24).** Yield: 79%; mp 119-121 °C. ¹H-NMR (DMSO-*d*₆, ppm, mixture of conformational isomers): 0.66-1.09 (m, 10H, Aliph-H); 1.22-1.35 (m, 4H, 2CH₂CH₂CH₂CH₃); 3.00-3.32 (m, 4H, 2NCH₂); 7.16-7.30 (m, 2H, Ar-H); 7.45-7.49 (m, 2H, Ar-H); 7.68-7.72 (m, 1H, Ar-H); 7.88-7.92 (m, 1H, 4-H); 8.11 (s, 1H, 2'-H); 12.43 (bs, 1H,

NH, exch. with D₂O). ¹³C-NMR (DMSO-*d*₆, ppm, mixture of conformational isomers): 13.82; 14.21; 19.66; 20.24; 29.41; 30.44; 43.98; 47.59; 109.85; 112.46; 120.93; 122.73; 123.86; 126.55; 127.04; 128.79; 129.23; 131.38; 136.04; 141.98; 168.37; 187.37. Anal. Calcd for C₂₂H₂₆N₂O₂S: C, 69.08; H, 6.85; N, 7.32. Found: C, 69.19; H, 6.76; N, 7.39.

***N,N*-Dihexyl-2-oxo-2-[2-(3-thienyl)-1*H*-indol-3-yl]acetamide (25).** Yield: 82%; oil. ¹H-NMR (DMSO-*d*₆, ppm, mixture of conformational isomers, mixture of conformational isomers): 0.66-1.12 (m, 14H, Aliph-H); 1.26-1.39 (m, 8H, Aliph-H); 3.00-3.20 (m, 4H, 2NCH₂); 7.18-7.29 (m, 2H, Ar-H); 7.45-7.51 (m, 2H, Ar-H); 7.68-7.72 (m, 1H, Ar-H); 7.87-7.93 (m, 1H, 4-H); 8.14 (s, 1H, 2'-H); 12.44 (bs, 1H, NH, exch. with D₂O). ¹³C-NMR (DMSO-*d*₆, ppm, mixture of conformational isomers): 14.17; 14.37; 22.21; 22.50; 25.98; 26.63; 27.22; 28.14; 31.00; 31.48; 44.23; 47.48; 109.76; 112.49; 120.88; 122.67; 123.82; 126.50; 127.02; 128.81; 129.21; 131.40; 136.07; 141.90; 168.43; 187.32. Anal. Calcd for C₂₆H₃₄N₂O₂S: C, 71.19; H, 7.81; N, 6.39. Found: C, 71.05; H, 7.89; N, 6.32.

2-(2-Biphenyl-4-yl-1*H*-indol-3-yl)-2-oxo-*N,N*-dipropylacetamide (26). Yield: 70%; mp 155-157 °C. ¹H-NMR (DMSO-*d*₆, ppm, mixture of conformational isomers): 0.67-0.73 (m, 6H, 2(CH₂)₂CH₃); 1.15-1.20, 1.45-1.51 (2m, 4H, 2CH₂CH₂CH₃); 2.92-3.10 (m, 4H, 2NCH₂); 7.29-7.32 (m, 2H, Ar-H); 7.51-7.55 (m, 4H, Ar-H); 7.68-7.81 (m, 6H, Ar-H); 8.06-8.08 (m, 1H, 4-H), 12.52 (bs, 1H, NH, exch. with D₂O). ¹³C-NMR (DMSO-*d*₆, ppm, mixture of conformational isomers): 11.40; 11.77; 20.93; 21.71; 46.01; 49.75; 110.29; 112.55; 121.31; 122.90; 123.91; 126.68; 127.24; 127.28; 128.39; 129.53; 130.33; 130.99; 136.26; 139.94; 141.80; 147.31; 168.02; 187.68. Anal. Calcd for C₂₈H₂₈N₂O₂: C, 79.22; H, 6.65; N, 6.60. Found: C, 79.56; H, 6.81; N, 6.44.

2-(2-Biphenyl-4-yl-1*H*-indol-3-yl)-*N,N*-dibutyl-2-oxoacetamide (27). Yield: 67%; mp 153-155 °C. ¹H-NMR (DMSO-*d*₆, ppm, mixture of conformational isomers): 0.71-0.78 (m, 6H, 2(CH₂)₃CH₃); 1.07-1.15 (m, 6H, Aliph-H); 1.41-1.44 (m, 2H, Aliph-H); 2.98-3.11 (m, 4H, 2NCH₂); 7.27-7.34 (m, 2H, Ar-H); 7.42-7.57 (m, 4H, Ar-H); 7.66-7.86 (m, 6H, Ar-H); 8.07-8.11 (m, 1H, 4-H); 12.51 (bs, 1H, NH, exch. with D₂O). ¹³C-NMR (DMSO-*d*₆, ppm, mixture of conformational

isomers): 13.93; 13.99; 19.72; 20.18; 29.08; 30.45; 43.95; 47.65; 110.27; 112.55; 121.33; 122.87; 123.90; 126.58; 127.18; 127.34; 128.40; 129.50; 130.33; 131.02; 136.33; 139.77; 141.64; 147.31; 167.93; 187.72. Anal. Calcd for C₃₀H₃₂N₂O₂: C, 79.61; H, 7.13; N, 6.19. Found: C, 79.91; H, 7.27; N, 5.92.

2-(2-Biphenyl-4-yl-1H-indol-3-yl)-N,N-dihexyl-2-oxoacetamide (28). Yield: 65%; mp 50-52 °C. ¹H-NMR (DMSO-*d*₆, ppm, mixture of conformational isomers): 0.72-0.75 (m, 6H, 2(CH₂)₅CH₃); 1.07-1.14 (m, 14H, Aliph-H); 1.41-1.44 (m, 2H, Aliph-H); 2.92-3.08 (m, 4H, 2NCH₂); 7.25-7.34 (m, 2H, Ar-H); 7.42-7.52 (m, 4H, Ar-H); 7.66-7.85 (m, 6H, Ar-H); 8.07-8.10 (m, 1H, 4-H), 12.51 (bs, 1H, NH, exch. with D₂O). ¹³C-NMR (DMSO-*d*₆, ppm, mixture of conformational isomers): 14.21; 14.24; 22.31; 22.48; 26.07; 26.69; 28.18; 31.13; 31.38; 39.40; 44.20; 47.84; 110.30; 112.51; 121.40; 122.86; 123.91; 126.55; 127.15; 127.33; 128.38; 129.47; 130.29; 131.04; 136.30; 139.70; 141.61; 147.26; 167.88; 187.77. Anal. Calcd for C₃₄H₄₀N₂O₂: C, 80.28; H, 7.93; N, 5.51. Found: C, 80.29; H, 8.15; N, 5.40.

2-[2-(2-Naphthyl)-1H-indol-3-yl]-2-oxo-N,N-dipropylacetamide (29). Yield: 60%; mp 171-172 °C. ¹H-NMR (DMSO-*d*₆, ppm, mixture of conformational isomers): 0.51, 0.71 (2t, *J* = 7.2 Hz, 6H, 2(CH₂)₂CH₃); 0.86-0.98, 1.41-1.52 (2m, 4H, 2CH₂CH₂CH₃); 2.79, 3.08 (2t, *J* = 7.0 Hz, 4H, 2NCH₂); 7.28-7.32 (m, 2H, Ar-H); 7.51-7.56 (m, 1H, Ar-H); 7.64-7.72 (m, 3H, Ar-H); 8.00-8.09 (m, 4H, Ar-H); 8.17 (s, 1H, 1'-H); 12.60 (bs, 1H, NH, exch. with D₂O). ¹³C-NMR (DMSO-*d*₆, ppm, mixture of conformational isomers): 11.39; 11.56; 20.18; 21.75; 45.94; 49.81; 110.46; 112.57; 121.33; 122.92; 123.94; 127.15; 127.29; 127.57; 127.60; 127.82; 128.07; 128.76; 128.85; 130.06; 132.65; 133.65; 136.35; 147.62; 168.00; 187.68. Anal. Calcd for C₂₆H₂₆N₂O₂: C, 78.36; H, 6.58; N, 7.03. Found: C, 78.49; H, 6.63; N, 6.95.

N,N-Dibutyl-2-[2-(2-naphthyl)-1H-indol-3-yl]-2-oxoacetamide (30). Yield: 79%; mp 98-100 °C. ¹H-NMR (DMSO-*d*₆, ppm, mixture of conformational isomers): 0.54, 0.75 (2t, *J* = 7.2 Hz, 6H, 2(CH₂)₃CH₃); 0.63-0.70, 0.83-0.90 (2m, 4H, 2(CH₂)₂CH₂CH₃); 1.09-1.14, 1.37-1.42 (2m, 4H, 2CH₂CH₂CH₂CH₃); 2.79, 3.09 (2t, *J* = 7.6 Hz, 4H, 2NCH₂); 7.27-7.35 (m, 2H, Ar-H); 7.50-7.53 (m,

1H, Ar-H); 7.60-7.70 (m, 3H, Ar-H); 8.00-8.05 (m, 3H, Ar-H); 8.11-8.14 (m, 1H, 4-H); 8.16 (s, 1H, 1'-H); 12.56 (bs, 1H, NH, exch. with D₂O). ¹³C-NMR (DMSO-*d*₆, ppm, mixture of conformational isomers): 13.89; 13.94; 19.72; 19.96; 28.78; 30.43; 43.81; 47.59; 110.55; 112.53; 121.43; 122.93; 123.96; 127.16; 127.34; 127.57; 127.59; 127.87; 128.14; 128.77; 130.20; 132.67; 133.68; 136.36; 147.66; 167.80; 187.83. Anal. Calcd for C₂₈H₃₀N₂O₂: C, 78.84; H, 7.09; N, 6.57. Found: C, 78.71; H, 7.05; N, 6.49.

***N,N*-Dihexyl-2-[2-(2-naphthyl)-1*H*-indol-3-yl]-2-oxoacetamide (31).** Yield: 88%; oil. ¹H-NMR (DMSO-*d*₆, ppm, mixture of conformational isomers): 0.70-0.88 (m, 10H, Aliph-H); 1.08-1.41 (m, 12H, Aliph-H); 2.82, 3.10 (2t, *J* = 7.6 Hz, 4H, 2NCH₂); 7.27-7.35 (m, 2H, Ar-H); 7.51-7.59 (m, 1H, Ar-H); 7.61-7.71 (m, 3H, Ar-H); 8.00-8.04 (m, 3H, Ar-H); 8.10-8.12 (m, 1H, 4-H); 8.16 (s, 1H, 1'-H); 12.57 (bs, 1H, NH, exch. with D₂O). ¹³C-NMR (DMSO-*d*₆, ppm, mixture of conformational isomers): 14.22; 14.31; 22.31; 22.36; 26.07; 26.41; 26.58; 28.18; 31.14; 31.19; 44.08; 47.82; 110.50; 112.54; 121.42; 122.89; 123.94; 127.14; 127.33; 127.57; 127.85; 128.12; 128.76; 130.20; 132.66; 133.66; 136.38; 147.61; 167.80; 187.82. Anal. Calcd for C₃₂H₃₈N₂O₂: C, 79.63; H, 7.94; N, 5.80. Found: C, 79.75; H, 7.97; N, 5.86.

***N*-Butyl-*N*-methyl-2-[2-(2-naphthyl)-1*H*-indol-3-yl]-2-oxoacetamide (32).** Yield: 70%; mp 74-76 °C. ¹H-NMR (DMSO-*d*₆, ppm, mixture of conformational isomers): 0.56-0.92 (m, 5H, (CH₂)₂CH₂CH₃); 1.12-1.56 (m, 2H, CH₂CH₂CH₂CH₃); 2.24, 2.82 (2s, 3H, NCH₃); 2.67, 3.13 (2t, *J* = 7.2 Hz, 2H, NCH₂); 7.29-7.36 (m, 2H, Ar-H); 7.51-7.55 (m, 1H, Ar-H); 7.61-7.69 (m, 3H, Ar-H); 8.01-8.05 (m, 3H, Ar-H); 8.15 (s, 1H, 1'-H); 8.17-8.19 (m, 1H, 4-H); 12.62 (bs, 1H, NH, exch. with D₂O). ¹³C-NMR (DMSO-*d*₆, ppm, mixture of conformational isomers): 13.89; 13.99; 19.60; 19.74; 28.08; 29.93; 31.04; 35.02; 45.49; 49.44; 110.57; 110.59; 112.56; 121.47; 121.51; 123.04; 124.02; 124.05; 127.18; 127.20; 127.27; 127.39; 127.46; 127.50; 127.63; 127.65; 127.86; 128.14; 128.66; 128.68; 128.74; 128.75; 129.92; 130.12; 132.53; 132.62; 133.56; 133.69; 136.33; 136.39; 147.83; 148.01; 167.48; 167.74; 187.78; 188.03. Anal. Calcd for C₂₅H₂₄N₂O₂: C, 78.10; H, 6.29; N, 7.29. Found: C, 78.23; H, 6.21; N, 7.32.

***N*-Methyl-2-[2-(2-naphthyl)-1*H*-indol-3-yl]-2-oxo-*N*-pentylacetamide (33).** Yield: 65%; mp 153-155 °C. ¹H-NMR (DMSO-*d*₆, ppm, mixture of conformational isomers): 0.70-1.00 (m, 7H, Aliph-H); 1.08-1.42 (m, 2H, CH₂CH₂(CH₂)₂CH₃); 2.25, 2.82 (2s, 3H, NCH₃); 2.66, 3.12 (2t, *J* = 7.2 Hz, 2H, NCH₂); 7.28-7.36 (m, 2H, Ar-H); 7.51-7.55 (m, 1H, Ar-H); 7.64-7.69 (m, 3H, Ar-H); 8.01-8.05 (m, 3H, Ar-H); 8.15 (s, 1H, 1'-H); 8.16-8.18 (m, 1H, 4-H); 12.60 (bs, 1H, NH, exch. with D₂O). ¹³C-NMR (DMSO-*d*₆, ppm, mixture of conformational isomers): 14.28; 14.23; 22.06; 22.14; 25.60; 27.42; 28.47; 28.72; 31.03; 35.04; 45.75; 49.65; 110.56; 110.59; 112.56; 121.46; 121.50; 123.04; 124.02; 124.05; 127.18; 127.26; 127.39; 127.44; 127.50; 127.61; 127.65; 127.86; 128.13; 128.67; 128.69; 128.74; 129.91; 130.12; 132.53; 132.62; 133.56; 133.67; 136.33; 136.39; 147.80; 148.01; 167.47; 167.76; 187.76; 188.01. Anal. Calcd for C₂₆H₂₆N₂O₂: C, 78.36; H, 6.58; N, 7.03. Found: C, 78.49; H, 6.62; N, 6.97.

***N*-Butyl-*N*-ethyl-2-[2-(2-naphthyl)-1*H*-indol-3-yl]-2-oxoacetamide (34).** Yield: 63%; mp 179-181 °C. ¹H-NMR (DMSO-*d*₆, ppm, mixture of conformational isomers): 0.53-1.04 (m, 10H, Aliph-H); 2.81-2.87 (m, 2H, Aliph-H); 3.20-3.33 (m, 2H, Aliph-H); 7.27-7.32 (m, 2H, Ar-H); 7.51-7.53 (m, 1H, Ar-H); 7.61-7.70 (m, 3H, Ar-H); 8.00-8.04 (m, 3H, Ar-H); 8.12-8.14 (m, 1H, 4-H); 8.15 (s, 1H, 1'-H); 12.58 (bs, 1H, NH, exch. with D₂O). ¹³C-NMR (DMSO-*d*₆, ppm, mixture of conformational isomers): 12.28; 13.91; 13.96; 14.02; 19.74; 19.95; 28.81; 30.54; 38.84; 42.58; 43.26; 47.47; 121.34; 121.44; 122.90; 123.92; 127.14; 127.16; 127.39; 127.45; 127.58; 127.80; 127.86; 128.10; 128.14; 128.75; 128.77; 128.89; 128.93; 130.10; 130.20; 132.64; 132.67; 133.61; 133.67; 136.52; 147.80; 147.98; 167.70; 187.66; 187.83. Anal. Calcd for C₂₆H₂₆N₂O₂: C, 78.36; H, 6.58; N, 7.03. Found: C, 78.49; H, 6.49; N, 7.07.

***N*-Benzyl-*N*-ethyl-2-[2-(2-naphthyl)-1*H*-indol-3-yl]-2-oxoacetamide (35).** Yield: 70%; mp 83-85 °C. ¹H-NMR (DMSO-*d*₆, ppm, mixture of conformational isomers): 0.26, 0.91 (2t, *J* = 7.0 Hz, 3H, CH₃); 2.73, 3.22 (2q, *J* = 7.0 Hz, 2H, NCH₂CH₃); 4.17, 4.41 (2s, 2H, NCH₂C₆H₅); 7.00-7.04 (m, 2H, Ar-H); 7.18-7.35 (m, 5H, Ar-H); 7.53-7.77 (m, 4H, Ar-H); 7.97-8.06 (m, 4H, Ar-H); 8.23-8.25 (m, 1H, 4-H); 12.65 (bs, 1H, NH, exch. with D₂O). ¹³C-NMR (DMSO-*d*₆, ppm, mixture of

conformational isomers): 11.47; 13.96; 38.40; 42.85; 46.73; 50.96; 110.02; 110.80; 112.62; 112.67; 121.22; 121.46; 122.96; 123.08; 123.98; 123.98; 124.08; 127.25; 127.38; 127.56; 127.59; 127.71; 127.83; 127.96; 128.14; 128.21; 128.27; 128.54; 128.74; 128.80; 128.83; 128.85; 130.07; 130.20; 132.66; 132.69; 133.67; 133.69; 136.42; 136.76; 137.36; 147.72; 148.17; 167.80; 168.39; 187.29; 187.68. Anal. Calcd for C₂₉H₂₄N₂O₂: C, 80.53; H, 5.59; N, 6.48. Found: C, 80.41; H, 5.49; N, 6.57.

General procedure for the synthesis of *N,N*-dialkyl-[2-(4-hydroxyphenyl)indol-3-yl]glyoxylamide derivatives 8-10. A stirred suspension of the appropriate derivative **17-19** (0.5 mmol) in 10 mL of dry dichloromethane was cooled to -10 °C and an excess (0.2 mL) of BBr₃ was added dropwise. The mixture was left under stirring for 30 min. at -10 °C, and subsequently at room temperature for 1h under nitrogen atmosphere. Finally, the solution was cooled again, and methanol (5 mL) was added to hydrolyze the excess of BBr₃. The solvent was evaporated at reduced pressure, and the solid precipitate was washed several times with methanol (3 x 5 mL). The residues obtained were purified by crystallization from toluene (compound **8**, 20 mL) or by flash chromatography (compounds **9** and **10**, ethyl acetate-petroleum ether 60-80 °C in varying v/v ratios as eluting system).

2-[2-(4-Hydroxyphenyl)-1*H*-indol-3-yl]-2-oxo-*N,N*-dipropylacetamide (8**).** Yield: 59%; mp 210-212 °C. ¹H-NMR (DMSO-*d*₆, ppm, mixture of conformational isomers): 0.64-0.82 (m, 6H, 2(CH₂)₂CH₃); 1.27-1.46 (m, 4H, 2CH₂CH₂CH₃); 2.95-3.02 (m, 4H, 2NCH₂); 6.86 (d, *J* = 8.4 Hz, 2H, 3'-H, 5'-H); 7.17-7.25 (m, 2H, Ar-H); 7.40-7.44 (m, 3H, Ar-H); 8.00-8.03 (m, 1H, 4-H); 9.90 (bs, 1H, OH, exch. with D₂O); 12.27 (bs, 1H, NH, exch. with D₂O). ¹³C NMR (DMSO-*d*₆, ppm, mixture of conformational isomers): 11.39; 11.84; 20.58; 21.72; 46.10; 49.82; 109.60; 112.32; 115.22; 121.15; 121.74; 122.63; 123.55; 127.40; 131.80; 136.08; 148.31; 159.32; 168.22; 187.64. Anal. Calcd for C₂₂H₂₄N₂O₃: C, 72.50; H, 6.64; N, 7.69. Found: C, 72.39; H, 6.59; N, 7.77.

***N,N*-Dibutyl-2-[2-(4-hydroxyphenyl)-1*H*-indol-3-yl]-2-oxoacetamide (**9**).** Yield: 68%; mp 250-252 °C. ¹H-NMR (DMSO-*d*₆, ppm, mixture of conformational isomers): 0.68-0.84 (m, 6H, 2(CH₂)₃CH₃); 1.02-1.35 (m, 8H, 2CH₂(CH₂)₂CH₃); 1.21-1.36, 2.96-2.99 (2m, 4H, 2NCH₂); 6.83 (d,

$J = 6.2$ Hz, 2H, 3'-H, 5'-H); 7.19-7.21 (m, 2H, Ar-H); 7.37-7.40 (m, 3H, Ar-H); 7.98-8.00 (m, 1H, 4-H); 9.84 (bs, 1H, OH, exch. with D₂O); 12.22 (bs, 1H, NH, exch. with D₂O). ¹³C-NMR (DMSO-*d*₆, ppm, mixture of conformational isomers): 13.99; 14.14; 19.75; 20.27; 29.50; 30.57; 44.07; 47.93; 111.04; 111.38; 115.25; 119.50; 121.55; 123.29; 123.83; 126.45; 132.47; 137.17; 149.73; 159.25; 167.54; 187.95. Anal. Calcd for C₂₄H₂₈N₂O₃: C, 73.44; H, 7.19; N, 7.14. Found: C, 73.59; H, 7.28; N, 7.26.

***N,N*-Dihexyl-2-[2-(4-hydroxyphenyl)-1*H*-indol-3-yl]-2-oxoacetamide (10).** Yield: 55%; oil. ¹H-NMR (DMSO-*d*₆, ppm, mixture of conformational isomers): 0.68-0.88 (m, 6H, 2(CH₂)₅CH₃); 1.04-1.23 (m, 16H, Aliph-H); 2.95-3.05 (m, 4H, 2NCH₂); 6.85 (d, $J = 8.4$ Hz, 2H, 3'-H, 5'-H); 7.18-7.22 (m, 2H, Ar-H); 7.38-7.45 (m, 3H, Ar-H); 7.97-8.00 (m, 1H, 4-H); 9.88 (bs, 1H, OH, exch. with D₂O); 12.27 (bs, 1H, NH, exch. with D₂O). ¹³C-NMR (DMSO-*d*₆, ppm, mixture of conformational isomers): 14.13; 14.23; 22.30; 22.56; 26.07; 26.71; 27.19; 28.21; 31.12; 31.47; 44.28; 47.81; 109.50; 112.24; 115.16; 121.20; 121.65; 122.54; 123.48; 127.37; 131.87; 136.06; 148.23; 159.34; 168.01; 187.90. Anal. Calcd for C₂₈H₃₆N₂O₃: C, 74.97; H, 8.09; N, 6.24. Found: C, 74.85; H, 7.98; N, 6.30.

General procedure for the synthesis of *N,N*-dialkyl-[2-(4-aminophenyl)indol-3-yl]glyoxylamide derivatives 11-13. Pd/C 10% (0.05 g) was added to a suspension of the appropriate derivative **7d-f**²⁶ (0.65 mmol) in 150 mL of absolute ethanol. The mixture was hydrogenated under stirring at room temperature. Once hydrogen absorption ceased, the catalyst was filtered off and the solution was evaporated to dryness at reduced pressure. The crude products obtained were finally purified by recrystallization from toluene (20-30 mL).

2-[2-(4-Aminophenyl)-1*H*-indol-3-yl]-2-oxo-*N,N*-dipropylacetamide (11). Yield: 62%; mp 197-199 °C. ¹H-NMR (DMSO-*d*₆, ppm, mixture of conformational isomers): 0.67, 0.81 (2t, $J = 7.2$ Hz, 6H, 2(CH₂)₂CH₃); 1.29-1.49 (m, 4H, 2CH₂CH₂CH₃); 2.97-3.08 (m, 4H, 2NCH₂); 5.57 (bs, 2H, NH₂, exch. with D₂O); 6.62 (d, $J = 8.4$ Hz, 2H, 3'-H, 5'-H); 7.17-7.43 (m, 5H, Ar-H); 7.92-7.97 (m, 1H, 4-H); 12.09 (bs, 1H, NH, exch. with D₂O). ¹³C-NMR (DMSO-*d*₆, ppm, mixture of

conformational isomers): 11.41; 11.89; 20.60; 21.67; 46.08; 49.77; 108.90; 112.14; 113.23; 117.84; 120.93; 122.39; 123.25; 127.64; 131.29; 136.10; 149.30; 150.87; 168.50; 187.45. Anal. Calcd for C₂₂H₂₅N₃O₂: C, 72.70; H, 6.93; N, 11.56. Found: C, 72.82; H, 6.87; N, 11.62.

2-[2-(4-Aminophenyl)-1H-indol-3-yl]-N,N-dibutyl-2-oxoacetamide (12). Yield: 61%; mp 225-227 °C; ¹H-NMR (DMSO-*d*₆, ppm, mixture of conformational isomers): 0.64, 0.87 (2t, *J* = 7.2 Hz, 6H, 2(CH₂)₃CH₃); 0.98-1.36 (m, 8H, 2CH₂(CH₂)₂CH₃); 3.00-3.06 (m, 4H, 2NCH₂); 5.52 (bs, 2H, NH₂, exch. with D₂O); 6.61 (d, *J* = 8.4 Hz, 2H, 3'-H, 5'-H); 7.15-7.41 (m, 5H, Ar-H); 7.93-7.96 (m, 1H, 4-H); 12.08 (bs, 1H, NH, exch. with D₂O). ¹³C-NMR (DMSO-*d*₆, ppm, mixture of conformational isomers): 13.88; 14.23; 19.72; 20.28; 29.34; 30.38; 43.90; 47.56; 108.92; 112.11; 113.22; 117.74; 120.97; 122.38; 123.27; 127.66; 131.35; 136.11; 149.33; 150.89; 168.34; 187.54. Anal. Calcd for C₂₄H₂₉N₃O₂: C, 73.63; H, 7.47; N, 10.73. Found: C, 73.52; H, 7.56; N, 10.79.

2-[2-(4-Aminophenyl)-1H-indol-3-yl]-N,N-dihexyl-2-oxoacetamide (13). Yield: 68%; mp 147-149 °C. ¹H-NMR (DMSO-*d*₆, ppm, mixture of conformational isomers): 0.68-0.89 (m, 6H, 2(CH₂)₃CH₃); 0.93-1.24 (m, 16H, Aliph-H); 2.97-3.12 (m, 4H, 2NCH₂); 5.58 (bs, 2H, NH₂, exch. with D₂O); 6.60 (d, *J* = 8.6 Hz, 2H, 3'-H, 5'-H); 7.16-7.41 (m, 5H, Ar-H); 7.90-7.93 (m, 1H, 4-H); 12.08 (bs, 1H, NH, exch. with D₂O). ¹³C-NMR (DMSO-*d*₆, ppm, mixture of conformational isomers): 14.20; 14.37; 22.26; 22.54; 26.05; 26.71; 27.19; 28.13; 31.08; 31.45; 44.21; 47.83; 108.82; 112.12; 113.33; 117.94; 120.90; 122.33; 123.23; 127.61; 131.35; 136.13; 149.22; 150.64; 168.42; 187.43. Anal. Calcd for C₂₈H₃₇N₃O₂: C, 75.13; H, 8.33; N, 9.39. Found: C, 75.02; H, 8.39; N, 9.28.

General procedure for the synthesis of N,N-dialkyl-[2-(4-carboxyphenyl)indol-3-yl]glyoxylamide derivatives 14-16. Lithium hydroxide monohydrate (0.3 mmol) was added to a suspension of the appropriate ester derivative **20-23** (0.5 mmol) in 20 mL of a MeOH/H₂O (3:1) solution. The mixture was stirred under reflux at 80 °C overnight. The solid precipitate was eliminated through vacuum filtration, and the solution was acidified with 10% HCl to pH 5. The acid precipitated was collected by filtration and did not need any further purification.

4-{3-[(Dipropylamino)(oxo)acetyl]-1H-indol-2-yl}benzoic acid (14). Yield: 85%; mp 292-294 °C. ¹H-NMR (DMSO-*d*₆, ppm, mixture of conformational isomers): 0.64-0.75 (m, 6H, 2(CH₂)₂CH₃); 1.15-1.26, 1.43-1.47 (2m, 4H, 2CH₂CH₂CH₃); 2.91-3.11 (m, 4H, 2NCH₂); 7.27-7.31 (m, 2H, Ar-H); 7.49-7.51 (m, 1H, Ar-H); 8.10 (d, *J* = 7.8 Hz, 2H, 3'-H, 5'-H); 8.03-8.07 (m, 3H, Ar-H); 12.63 (bs, 1H, NH, exch. with D₂O). ¹³C-NMR (DMSO-*d*₆, ppm, mixture of conformational isomers): 11.38; 11.73; 20.43; 21.76; 46.03; 49.78; 110.48; 112.69; 121.32; 123.05; 124.12; 127.09; 129.24; 130.64; 132.10; 135.51; 136.31; 146.27; 167.40; 167.89; 187.50. Anal. Calcd for C₂₃H₂₄N₂O₄: C, 70.39; H, 6.16; N, 7.14. Found: C, 70.22; H, 6.25; N, 7.18.

4-{3-[(Dibutylamino)(oxo)acetyl]-1H-indol-2-yl}benzoic acid (15). Yield: 87%; mp 148-150 °C. ¹H-NMR (DMSO-*d*₆, ppm, mixture of conformational isomers): 0.68-0.81 (m, 6H, 2(CH₂)₃CH₃); 1.03-1.40 (m, 8H, 2CH₂(CH₂)₂CH₃); 2.93-3.04 (m, 4H, 2NCH₂); 7.25-7.28 (m, 2H, Ar-H); 7.46-7.50 (m, 1H, Ar-H); 7.68 (d, *J* = 6.8 Hz, 2H, 3'-H, 5'-H); 8.00-8.08 (m, 3H, Ar-H); 12.56 (bs, 1H, NH, exch. with D₂O). ¹³C-NMR (DMSO-*d*₆, ppm, mixture of conformational isomers): 13.91; 14.07; 19.70; 20.17; 29.09; 30.42; 43.93; 47.57; 110.57; 112.65; 121.44; 123.05; 124.14; 127.17; 129.31; 130.71; 132.11; 135.48; 136.33; 146.32; 167.37; 167.68; 187.64. Anal. Calcd for C₂₅H₂₈N₂O₄: C, 71.41; H, 6.71; N, 6.66. Found: C, 71.27; H, 6.79; N, 6.57.

4-{3-[(Dihexylamino)(oxo)acetyl]-1H-indol-2-yl}benzoic acid (16). Yield: 79%; mp 242-244 °C. ¹H-NMR (DMSO-*d*₆, ppm, mixture of conformational isomers): 0.73-0.84 (m, 6H, 2(CH₂)₅CH₃); 1.00-1.38 (m, 16H, Aliph-H); 2.93-3.03 (m, 4H, 2NCH₂); 7.24-7.27 (m, 2H, Ar-H); 7.46-7.50 (m, 1H, Ar-H); 7.68 (d, *J* = 7.8 Hz, 2H, 3'-H, 5'-H); 8.00-8.05 (m, 3H, Ar-H); 12.56 (bs, 1H, NH, exch. with D₂O). ¹³C-NMR (DMSO-*d*₆, ppm, mixture of conformational isomers): 14.20; 14.32; 22.29; 22.48; 26.04; 26.59; 26.88; 28.17; 31.10; 31.38; 44.19; 47.80; 110.53; 112.64; 121.42; 123.01; 124.12; 127.15; 129.28; 130.70; 132.09; 135.47; 136.35; 146.25; 167.33; 167.70; 187.63. Anal. Calcd for C₂₉H₃₆N₂O₄: C, 73.08; H, 7.61; N, 5.88. Found: C, 72.95; H, 7.71; N, 5.96.

Biological Methods. Materials. [³H]PK11195 (S.A. 85.5 Ci/mmol) and [³H]Ro15-1788 (S.A. 83.4 Ci/mmol) were purchased from Perkin-Elmer Life Sciences. Culture medium, fetal bovine serum

(FBS), L-glutamine, and antibiotics were purchased from Euroclone SpA (Milano, Italy). PK11195 and Ro5-4864 were obtained from Sigma-Aldrich. All other reagents were obtained from commercial suppliers.

[³H]PK11195 Binding to Rat Kidney Mitochondrial Membranes. For binding studies, crude mitochondrial membranes were incubated with 0.5 nM [³H]PK11195 in the presence of a compound concentration range (1 pM to 10 μM) in 50 mM Tris-HCl, pH 7.4, as previously described.^{25,26} For the active compounds, the IC₅₀ values were determined and K_i values were derived in accordance with the equation of Cheng and Prusoff.⁴²

[³H]Ro15-1788 Binding to Rat Cerebral Cortex Membranes. Rat cerebral cortex membranes were prepared as previously described.² After differential centrifugation, the crude membrane fraction obtained was subjected to washing procedures to remove endogenous GABA.⁴³ The washed membranes were incubated with 0.4 nM [³H]Ro15-1788 for 90 min at 0 °C in 500 μL of 50 mM Tris-citrate buffer, pH 7.4, as previously described.⁴⁴

Computational Studies. *Homology Modeling.* Recently the group of Zweckstetter released the NMR structure of the mouse TSPO (mTSPO) in complex with the PK11195 modulator,⁵ thus, paving the way for a better definition of the interaction mode between TSPO and its synthetic modulators. Our group in the last decades embarked in the discovery of new promising TSPO modulators, describing different ligand classes able to interact with rat TSPO (rTSPO) at the sub-nanomolar range, with the indolyglyoxylamide class being the most promising one.^{25-27,29,30} mTSPO and rTSPO share a 95% sequence identity, making mTSPO a suitable template for homology modeling approaches. Therefore, we decided to build a three-dimensional (3D) rTSPO model by using the Modeller9.13 software, and mTSPO as template (See Supplementary Figure S6 for the sequence alignment). The final rTSPO model was subsequently used to perform docking studies and to rationalize the SARs of the new series of indolyglyoxylamide derivatives described herein.

Docking studies. The selected 20 rTSPO models were used to dock the new series of indolylglyoxylamide derivatives reported in this work. All the docking studies were performed employing the Glide tool implemented in Maestro9.8.³⁶ The ligand used for the validation step of the rTSPO structures was represented by our lead in the new series of the indolylglyoxylamide (**Chart 1**, compound **29**, Table 2). The 3D structures of **29** was generated with the Maestro fragment Build tool and then geometrically optimized with Macromodel.³⁶ The rTSPO structures were prepared through the Protein Preparation Wizard of the Maestro 9.8³⁶ graphical user interface which assigns bond orders, adds hydrogen atoms, and generates appropriate protonation states. The docking grid box was centered on the residues lining the PK11195 binding pocket, with a grid box dimension equal to 24 x 24 x 24 Å (See Supplementary Figure S7). In detail the residues considered to center the docking grid are: A23, V26, L49, A50, I52, W107, V110, L114, A147, and L150 (which are conserved between the mTSPO and rTSPO, a part A110V). Finally, docking runs were carried out using the standard precision (SP) method. Finally, all the compounds reported in Tables 1-2 were docked using the refined rTSPO-**29** complex applying the same docking protocol.

■ ASSOCIATED CONTENT

Supporting Information Available. Biological Methods for evaluation of steroidogenic activity of compound **29**; Supplementary Figures S1-S7. This material is available free of charge via the Internet at <http://pubs.acs.org>.

■ AUTHOR INFORMATION

Corresponding Author. *Sabrina Taliani, Phone: +39-0502219547, Fax: +39-0502219605, E-mail: sabrina.taliani@farm.unipi.it; *Sandro Cosconati, Phone: +39-0823274789, Fax: +39-0823274605, E-mail: sandro.cosconati@unina2.it.

¥ These Authors contributed equally

■ ACKNOWLEDGMENTS

This study was financially supported by MIUR (Futuro in Ricerca 2010, PRIN 2010-2011), University of Pisa.

■ ABBREVIATIONS USED

BzR, central benzodiazepine receptor; CNS, central nervous system; SAR, structure-affinity relationships; TSPO, Translocator Protein.

REFERENCES

- [1] Papadopoulos, V.; Baraldi, M.; Guilarte, T. R.; Knudsen, T. B.; Lacapere, J. J.; Lindemann, P.; Norenberg, M. D.; Nutt, D.; Weizman, A.; Zhang, M. R.; Gavish, M. Translocator protein (18 kDa): new nomenclature for the peripheral-type benzodiazepine receptor based on its structure and molecular function. *Trends Pharmacol. Sci.* **2006**, *27*, 402-409.
- [2] Squires, R. F.; Braestrup, C. Benzodiazepine receptors in rat brain. *Nature* **1977**, *266*, 732-734.
- [3] Bouyer, G.; Cueff, A.; Egee, S.; Kmiecik, J.; Maksimova, Y.; Glogowska, E.; Gallagher, P. G.; Thomas, S. L. Erythrocyte peripheral type benzodiazepine receptor/voltage-dependent anion channels are upregulated by Plasmodium falciparum. *Blood* **2011**, *118*, 2305-2312.
- [4] Fan, J.; Lindemann, P.; Feuilleley, M. G.; Papadopoulos, V. Structural and functional evolution of the translocator protein (18 kDa). *Curr. Mol. Med.* **2012**, *12*, 369-386.
- [5] Jaremko, L.; Jaremko, M.; Giller, K.; Becker, S.; Zweckstetter, M. Structure of the mitochondrial translocator protein in complex with a diagnostic ligand. *Science* **2014**, *343*, 1363-1366.
- [6] Veenman, L.; Gavish, M. The role of 18 kDa mitochondrial translocator protein (TSPO) in programmed cell death, and effects of steroids on TSPO expression. *Curr. Mol. Med.* **2012**, *12*, 398-412.

- [7] Venneti, S.; Wang, G.; Nguyen, J.; Wiley, C. A. The positron emission tomography ligand DAA1106 binds with high affinity to activated microglia in human neurological disorders. *J. Neuropathol. Exp. Neurol.* **2008**, *67*, 1001-1010.
- [8] Rone, M. B.; Fan, J.; Papadopoulos, V. Cholesterol transport in steroid biosynthesis: role of protein-protein interactions and implications in disease states. *Biochim. Biophys. Acta* **2009**, *1791*, 646-658.
- [9] Nothdurfter, C.; Rammes, G.; Baghai, T. C.; Schule, C.; Schumacher, M.; Papadopoulos, V.; Rupprecht, R. Translocator protein (18 kDa) as a target for novel anxiolytics with a favourable side-effect profile. *J. Neuroendocrinol.* **2012**, *24*, 82-92.
- [10] Batarseh, A.; Papadopoulos, V. Regulation of translocator protein 18 kDa (TSPO) expression in health and disease states. *Mol. Cell. Endocrinol.* **2010**, *327*, 1-12.
- [11] Trapani, A.; Palazzo, C.; de Candia, M.; Lasorsa, F. M.; Trapani, G. Targeting of the translocator protein 18 kDa (TSPO): a valuable approach for nuclear and optical imaging of activated microglia. *Bioconjugate Chem.* **2013**, *24*, 1415-1428.
- [12] Austin, C. J.; Kahlert, J.; Kassiou, M.; Rendina, L. M. The translocator protein (TSPO): a novel target for cancer chemotherapy. *Int. J. Biochem. Cell. Biol.* **2013**, *45*, 1212-1216.
- [13] Girard, C.; Liu, S.; Adams, D.; Lacroix, C.; Sineus, M.; Boucher, C.; Papadopoulos, V.; Rupprecht, R.; Schumacher, M.; Groyer, G. Axonal regeneration and neuroinflammation: roles for the translocator protein 18 kDa. *J. Neuroendocrinol.* **2012**, *24*, 71-81.
- [14] Costa, B.; Da Pozzo, E.; Martini, C. Translocator protein as a promising target for novel anxiolytics. *Curr. Top. Med. Chem.* **2012**, *12*, 270-285.
- [15] Le Fur, G.; Vaucher, N.; Perrier, M. L.; Flamier, A.; Benavides, J.; Renault, C.; Dubroeuq, M. C.; Gueremy, C.; Uzan, A. Differentiation between two ligands for peripheral benzodiazepine binding sites, [³H]Ro5-4864 and [³H]PK11195, by thermodynamic studies. *Life Sci.* **1983**, *33*, 449-457.

- [16] Romeo, E.; Auta, J.; Kozikowski, A. P.; Ma, D.; Papadopoulos, V.; Puia, G.; Costa, E.; Guidotti, A. 2-Aryl-3-indoleacetamides (FGIN-1): a new class of potent and specific ligands for the mitochondrial DBI receptor (MDR). *J. Pharmacol. Exp. Ther.* **1992**, *262*, 971–978.
- [17] Wadsworth, H.; Jones, P. A.; Chau, W. F.; Durrant, C.; Fouladi, N.; Passmore, J.; O'Shea, D.; Wynn, D.; Morisson-Iveson, V.; Ewan, A.; Thaning, M.; Mantzilas, D.; Gausemel, I.; Khan, I.; Black, A.; Avory, M.; Trigg, W. [¹⁸F]GE-180: a novel fluorine-18 labelled PET tracer for imaging Translocator protein 18 kDa (TSPO). *Bioorg. Med. Chem. Lett.* **2012**, *22*, 1308-1313.
- [18] Boutin, H.; Murray, K.; Pradillo, J.; Maroy, R.; Smigova, A.; Gerhard, A.; Jones, P. A.; Trigg, W. ¹⁸F-GE-180: a novel TSPO radiotracer compared to ¹¹C-R-PK11195 in a preclinical model of stroke. *Eur. J. Nucl. Med. Mol. Imaging* **2015**, *42*, 503-511.
- [19] Trigg, W.; Jones, P. A. Preparation of carbazoles as TSPO-binding radiotracers. PCT Int. Appl. WO2015040148 A1 20150326, **2015**.
- [20] Kita, A.; Kohayakawa, H.; Kinoshita, T.; Ochi, Y.; Nakamichi, K.; Kurumiya, S.; Furukawa, K.; Oka, M. Antianxiety and antidepressant-like effects of AC-5216, a novel mitochondrial benzodiazepine receptor ligand. *Br. J. Pharmacol.* **2004**, *142*, 1059–1072.
- [21] James, M. L.; Selleri, S.; Kassiou, M. Development of ligands for the peripheral benzodiazepine receptor. *Curr. Med. Chem.* **2006**, *13*, 1991-2001.
- [22] Taliani, S.; Da Settimo, F.; Da Pozzo, E.; Chelli, B.; Martini, C. Translocator protein ligands as promising therapeutic tools for anxiety disorders. *Curr. Med. Chem.* **2009**, *16*, 3359-3380.
- [23] Scarf, A. M.; Ittner, L. M.; Kassiou, M. The translocator protein (18 kDa): central nervous system disease and drug design. *J. Med. Chem.* **2009**, *52*, 581-592.
- [24] Taliani, S.; Pugliesi, I.; Da Settimo, F. Structural requirements to obtain highly potent and selective 18 kDa translocator protein (TSPO) ligands. *Curr. Top. Med. Chem.* **2011**, *11*, 860-886.
- [25] Primofiore, G.; Da Settimo, F.; Taliani, S.; Simorini, F.; Patrizi, M. P.; Novellino, E.; Greco, G.; Abignente, E.; Costa, B.; Chelli, B.; Martini, C. *N,N*-dialkyl-2-phenylindol-3-ylglyoxylamides.

A new class of potent and selective ligands at the peripheral benzodiazepine receptor. *J. Med. Chem.* **2004**, *47*, 1852-1855.

[26] Da Settimo, F.; Simorini, F.; Taliani, S.; La Motta, C.; Marini, A. M.; Salerno, S.; Bellandi, M.; Novellino, E.; Greco, G.; Cosimelli, B.; Da Pozzo, E.; Costa, B.; Simola, N.; Morelli, M.; Martini, C. Anxiolytic-like effects of *N,N*-dialkyl-2-phenylindol-3-ylglyoxylamides by modulation of translocator protein promoting neurosteroid biosynthesis. *J. Med. Chem.* **2008**, *51*, 5798-5806.

[27] Simorini, F.; Marini, A. M.; Taliani, S.; La Motta, C.; Salerno, S.; Pugliesi, I.; Da Settimo, F. Medicinal chemistry of indolyglyoxylamide TSPO high affinity ligands with anxiolytic-like effects. *Curr. Top. Med. Chem.* **2012**, *12*, 333-351.

[28] Campiani, G.; Nacci, V.; Fiorini, I.; De Filippis, M. P.; Garofalo, A.; Ciani, S. M.; Greco, G.; Novellino, E.; Williams, D. C.; Zisterer, D. M.; Woods, M. J.; Mihai, C.; Manzoni, C.; Mennini, T. Synthesis, biological activity, and SARs of pyrrolobenzoxazepine derivatives, a new class of specific "peripheral-type" benzodiazepine receptor ligands. *J. Med. Chem.* **1996**, *39*, 3435-3450.

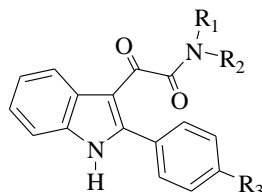
[29] (a) Taliani, S.; Simorini, F.; Sergianni, V.; La Motta, C.; Da Settimo, F.; Cosimelli, B.; Abignente, E.; Greco, G.; Novellino, E.; Rossi, L.; Gremigni, V.; Spinetti, F.; Chelli, B.; Martini, C. New fluorescent 2-phenylindolglyoxylamide derivatives as probes targeting the peripheral-type benzodiazepine receptor: design, synthesis, and biological evaluation. *J. Med. Chem.* **2007**, *50*, 404-407. (b) Taliani, S.; Da Pozzo, E.; Bellandi, M.; Bendinelli, S.; Pugliesi, I.; Simorini, F.; La Motta, C.; Salerno, S.; Marini, A. M.; Da Settimo, F.; Cosimelli, B.; Greco, G.; Novellino, E.; Martini, C. Novel irreversible fluorescent probes targeting the 18 kDa translocator protein: synthesis and biological characterization. *J. Med. Chem.* **2010**, *53*, 4085-4093.

[30] (a) Kenner, R. A.; Aboderin, A. A. New fluorescent probe for protein and nucleoprotein conformation. Binding of 7-(*p*-methoxybenzylamino)-4-nitrobenzoxadiazole to bovine trypsinogen and bacterial ribosomes. *Biochemistry* **1971**, *10*, 4433-4440. (b) Uchiyama, S.; Santa, T.; Imai, K. Fluorescence characteristics of six 4,7-disubstituted benzofurazan compounds: an experimental and semi-empirical MO study. *J. Chem. Soc. Perkin Trans.* **1999** *2*, 2525-2532.

- [31] Pike, V. W.; Taliani, S.; Lohith, T. G.; Owen, D. R. J.; Pugliesi, I.; Da Pozzo, E.; Hong, J.; Zoghbi, S. S.; Gunn, R. N.; Parker, C. A.; Rabiner, E. A.; Fujita, M.; Innis, R. B.; Martini, C.; Da Settimo, F. Evaluation of novel N¹-methyl-2-phenylindol-3-ylglyoxylamides as a new chemotype of 18 kDa translocator protein-selective ligand suitable for the development of positron emission tomography radioligands. *J. Med. Chem.* **2011**, *54*, 366-373.
- [32] Denora, N.; Laquintana, V.; Pisu, M. G.; Dore, R.; Murru, L.; Latrofa, A.; Trapani, G.; Sanna, E. 2-Phenyl-imidazo[1,2-a]pyridine compounds containing hydrophilic groups as potent and selective ligands for peripheral benzodiazepine receptors: synthesis, binding affinity and electrophysiological studies. *J. Med. Chem.* **2008**, *51*, 6876-6888.
- [33] Guo, Y.; Kalathur, R. C.; Liu, Q.; Kloss, B.; Bruni, R.; Ginter, C.; Kloppmann, E.; Rost, B.; Hendrickson, W. A. Structure and activity of tryptophan-rich TSPO proteins. *Science* **2015**, *347*, 551-555.
- [34] Li, F.; Liu, J.; Zheng, Y.; Garavito, R. M.; Ferguson-Miller, S. Protein structure. Crystal structures of translocator protein (TSPO) and mutant mimic of a human polymorphism. *Science* **2015**, *347*, 555-558.
- [35] Bernstein, F. C.; Koetzle, T. F.; Williams, G. J. B.; Meyer Jr., E. F.; Brice, M.D.; Rodgers, J. R.; Kennard, O.; Shimanouchi, T.; Tasumi, M. The Protein Data Bank: a computer-based archival file for macromolecular structures. *J. Mol. Biol.* **1977**, *112*, 535-542.
- [36] Schrödinger, Maestro version 9.8 Schrödinger, LLC, New York <http://www.schrodinger.com/>. **2014**.
- [37] Castellano, S.; Taliani, S.; Viviano, M.; Milite, C.; Da Pozzo, E.; Costa, B.; Barresi, E.; Bruno, A.; Cosconati, S.; Marinelli, L.; Greco, G.; Novellino, E.; Sbardella, G.; Da Settimo, F.; Martini, C. Structure-activity relationship refinement and further assessment of 4-phenylquinazoline-2-carboxamide translocator protein ligands as antiproliferative agents in human glioblastoma tumors. *J. Med. Chem.* **2014**, *57*, 2413-2428.

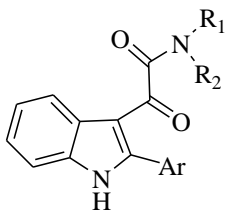
- [38] Anzini, M.; Cappelli, A.; Vomero, S.; Seeber, M.; Menziani, M. C.; Langer, T.; Hagen, B.; Manzoni, C.; Bourguignon, J. J. Mapping and fitting the peripheral benzodiazepine receptor binding site by carboxamide derivatives. Comparison of different approaches to quantitative ligand-receptor interaction modeling. *J. Med. Chem.* **2001**, *44*, 1134-1150.
- [39] Karaaslan, C.; Kadri, H.; Coban, T.; Suzen, S.; Westwell, A. D. Synthesis and antioxidant properties of substituted 2-phenyl-1*H*-indoles. *Bioorg. Med. Chem. Lett.* **2013**, *23*, 2671-2674.
- [40] Tsuchimoto, T.; Matsubayashi, H.; Kaneko, M.; Nagase, Y.; Miyamura, T.; Shirakawa, E. Iridium-catalyzed annulation of 2-aryl- and 2-heteroarylindoles with propargyl ethers: concise synthesis and photophysical properties of diverse aryl- and heteroaryl-annulated[*a*]carbazoles. *J. Am. Chem. Soc.* **2008**, *130*, 15823-15835.
- [41] Ackermann, L.; Barfuesser, S.; Potukuchi, H. K. Copper-catalyzed *N*-arylation/hydroamin(d)ation domino synthesis of indoles and its application to the preparation of a Chek1/KDR kinase inhibitor pharmacophore. *Adv. Synth. Catal.* **2009**, *351*, 1064-1072.
- [42] Cheng, Y.; Prusoff, W. H. Relationship between the inhibition constant (K_1) and the concentration of inhibitor which causes 50 per cent inhibition (I_{50}) of an enzymatic reaction. *Biochem. Pharmacol.* **1973**, *22*, 3099-3108.
- [43] Karobath, M.; Sperk, G. Stimulation of benzodiazepine receptor binding by gamma-aminobutyric acid. *Proc. Natl. Acad. Sci. USA* **1979**, *76*, 1004-1006.
- [44] Taliani, S.; Cosimelli, B.; Da Settimo, F.; Marini, A. M.; La Motta, C.; Simorini, F.; Salerno, S.; Novellino, E.; Greco, G.; Cosconati, S.; Marinelli, L.; Salvetti, F.; L'Abbate, G.; Trasciatti, S.; Montali, M.; Costa, B.; Martini, C. Identification of anxiolytic/nonsedative agents among indol-3-ylglyoxylamides acting as functionally selective agonists at the gamma-aminobutyric acid-A ($GABA_A$) α_2 benzodiazepine receptor. *J. Med. Chem.* **2009**, *52*, 3723-3734.

Table 1. TSPO Binding Affinity of *N,N*-Dialkyl-2-(4'-substitutedphenyl)indol-3-ylglyoxylylamide Derivatives **8-22**, **7a-f**.



compd	R ₁ = R ₂	R ₃	K _i (nM) ^a
8	(CH ₂) ₂ CH ₃	OH	16.1 ± 1.0
9	(CH ₂) ₃ CH ₃	OH	25.7 ± 2.6
10	(CH ₂) ₅ CH ₃	OH	6.3 ± 0.5
11	(CH ₂) ₂ CH ₃	NH ₂	44.4 ± 5.0
12	(CH ₂) ₃ CH ₃	NH ₂	133 ± 13
13	(CH ₂) ₅ CH ₃	NH ₂	4.2 ± 0.4
14	(CH ₂) ₂ CH ₃	COOH	343 ± 10
15	(CH ₂) ₃ CH ₃	COOH	406 ± 4
16	(CH ₂) ₅ CH ₃	COOH	184 ± 1
17	(CH ₂) ₂ CH ₃	OCH ₃	5.8 ± 0.5
18	(CH ₂) ₃ CH ₃	OCH ₃	20.3 ± 2.2
19	(CH ₂) ₅ CH ₃	OCH ₃	4.0 ± 0.4
20	(CH ₂) ₂ CH ₃	COOCH ₃	3.1 ± 0.3
21	(CH ₂) ₃ CH ₃	COOCH ₃	2.7 ± 0.3
22	(CH ₂) ₅ CH ₃	COOCH ₃	3.3 ± 0.3
7a^b	(CH ₂) ₂ CH ₃	H	12.2 ± 1.0
7b^b	(CH ₂) ₃ CH ₃	H	7.5 ± 0.7
7c^b	(CH ₂) ₅ CH ₃	H	1.4 ± 0.2
7d^b	(CH ₂) ₂ CH ₃	NO ₂	0.95 ± 0.10
7e^b	(CH ₂) ₃ CH ₃	NO ₂	0.27 ± 0.10
7f^b	(CH ₂) ₅ CH ₃	NO ₂	0.23 ± 0.10
Ro5-4864 (1)			23.0 ± 3.1
PK11195 (2)			9.3 ± 0.5

^aThe concentration of tested compounds that inhibited [³H]PK11195 binding to rat kidney mitochondrial membranes by 50% (IC₅₀) was determined with eight concentrations of the displacers, each performed in triplicate. K_i values are the means ± SEM of three determinations. ^bData taken from ref. n. 26.

Table 2. TSPO Binding Affinity of *N,N*-Dialkyl-2-arylindol-3-ylglyoxylylamide Derivatives **23-35**, **7a-c**, **g-****j.**

cmpd	R ₁	R ₂	Ar	K _i (nM) ^a
23	(CH ₂) ₂ CH ₃	(CH ₂) ₂ CH ₃	thien-3-yl	1.2 ± 0.1
24	(CH ₂) ₃ CH ₃	(CH ₂) ₃ CH ₃	thien-3-yl	2.8 ± 0.3
25	(CH ₂) ₅ CH ₃	(CH ₂) ₅ CH ₃	thien-3-yl	0.89 ± 0.10
26	(CH ₂) ₂ CH ₃	(CH ₂) ₂ CH ₃	<i>p</i> -biphenyl	0.53 ± 0.05
27	(CH ₂) ₃ CH ₃	(CH ₂) ₃ CH ₃	<i>p</i> -biphenyl	5.5 ± 1.0
28	(CH ₂) ₅ CH ₃	(CH ₂) ₅ CH ₃	<i>p</i> -biphenyl	1.8 ± 0.2
29	(CH ₂) ₂ CH ₃	(CH ₂) ₂ CH ₃	naphth-2-yl	0.31 ± 0.04
30	(CH ₂) ₃ CH ₃	(CH ₂) ₃ CH ₃	naphth-2-yl	0.54 ± 0.06
31	(CH ₂) ₅ CH ₃	(CH ₂) ₅ CH ₃	naphth-2-yl	0.52 ± 0.06
32	CH ₃	(CH ₂) ₃ CH ₃	naphth-2-yl	0.56 ± 0.06
33	CH ₃	(CH ₂) ₄ CH ₃	naphth-2-yl	0.37 ± 0.04
34	CH ₂ CH ₃	(CH ₂) ₃ CH ₃	naphth-2-yl	0.51 ± 0.05
35	CH ₂ CH ₃	CH ₂ C ₆ H ₅	naphth-2-yl	0.51 ± 0.05
7a^b	(CH ₂) ₂ CH ₃	(CH ₂) ₂ CH ₃	C ₆ H ₅	12.2 ± 1.0
7b^b	(CH ₂) ₃ CH ₃	(CH ₂) ₃ CH ₃	C ₆ H ₅	7.5 ± 0.7
7c^b	(CH ₂) ₅ CH ₃	(CH ₂) ₅ CH ₃	C ₆ H ₅	1.4 ± 0.2
7g^b	CH ₃	(CH ₂) ₃ CH ₃	C ₆ H ₅	53.3 ± 4.0
7h^b	CH ₃	(CH ₂) ₄ CH ₃	C ₆ H ₅	12.1 ± 1.0
7i^b	CH ₂ CH ₃	(CH ₂) ₃ CH ₃	C ₆ H ₅	12.6 ± 1.0
7j^b	CH ₂ CH ₃	CH ₂ C ₆ H ₅	C ₆ H ₅	11.0 ± 1.0
Ro5-4864 (1)				23.0 ± 3.1
PK11195 (2)				9.3 ± 0.5

^aThe concentration of tested compound that inhibited [³H]PK11195 binding to rat kidney mitochondrial membranes by 50% (IC₅₀) was determined with eight concentrations of the displacers, each performed in triplicate. K_i values are the means ± SEM of three determinations. ^bData taken from ref. n. 26.

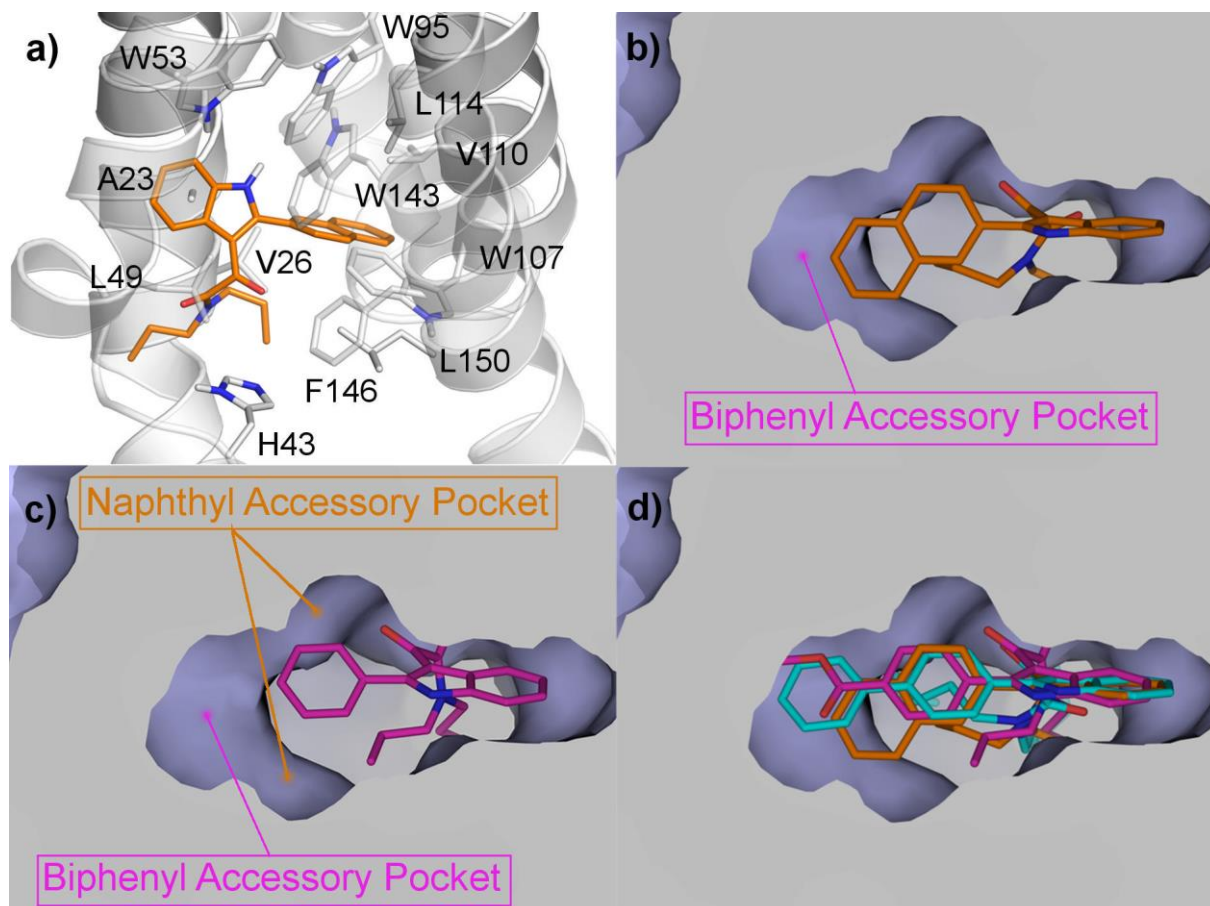
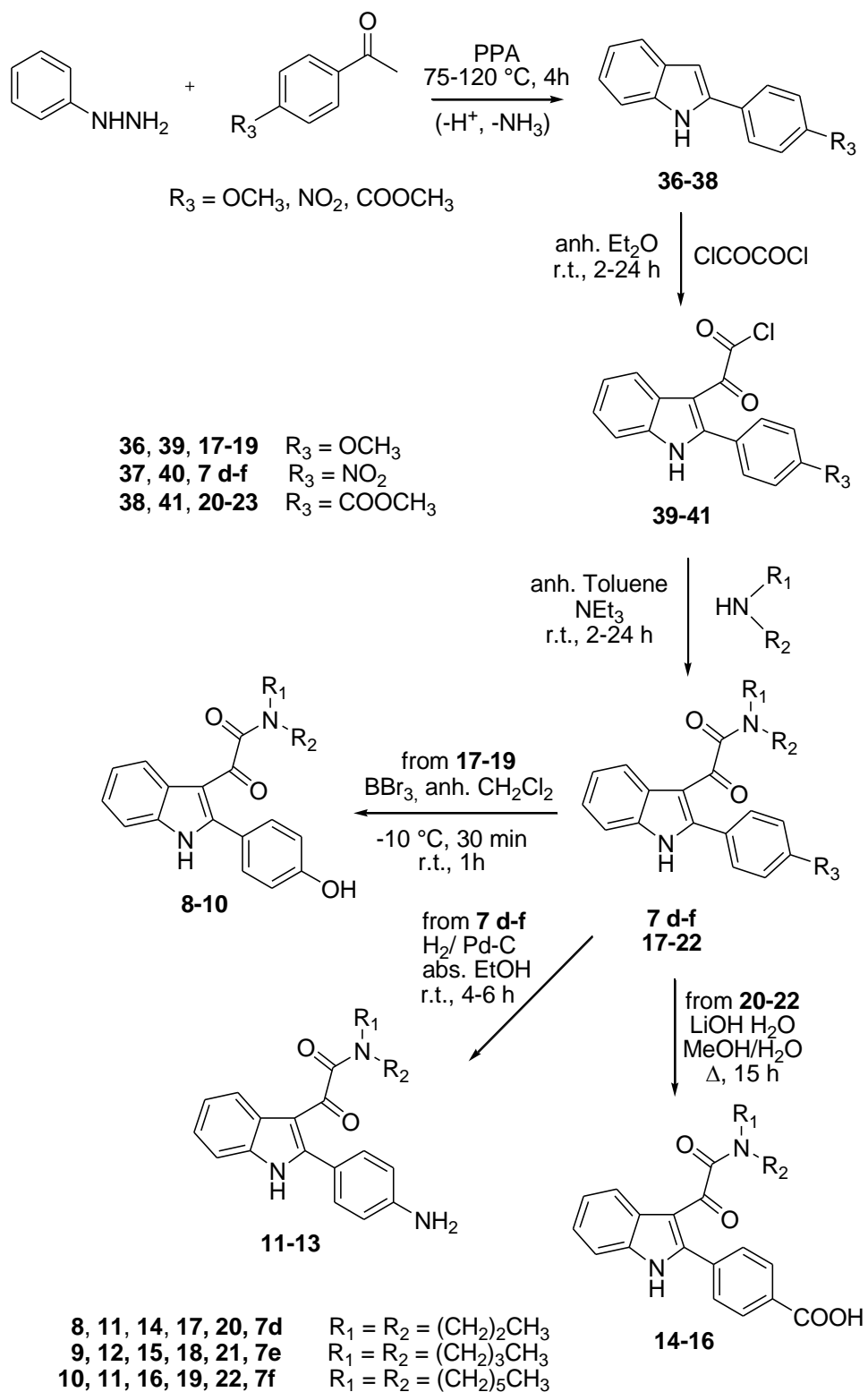
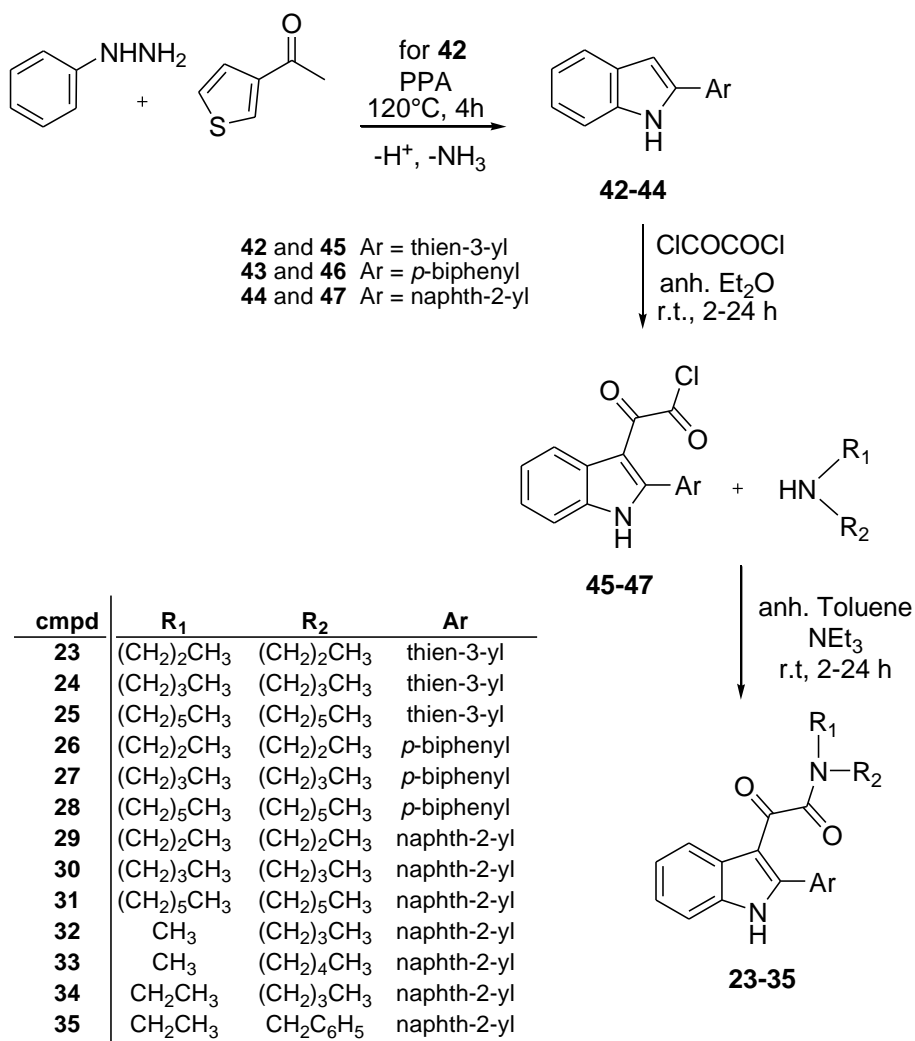


Figure 1. a) Binding mode of **29** (orange sticks) into the rTSPO binding site (white cartoon and sticks). b) Bottom view of **29** binding mode, (the TSPO structure is highlighted in blue and gray surfaces in this as well as in pictures c and d). c) Bottom view of **7a** binding mode. d) Bottom view of **29** (orange sticks), **20** (purple sticks), and **26** (cyan sticks) binding modes.



Scheme 1. Synthesis of indolyglyoxylamide derivatives **8-16**.



Scheme 2. Synthesis of indolylglyoxylamide derivatives **23-35**.

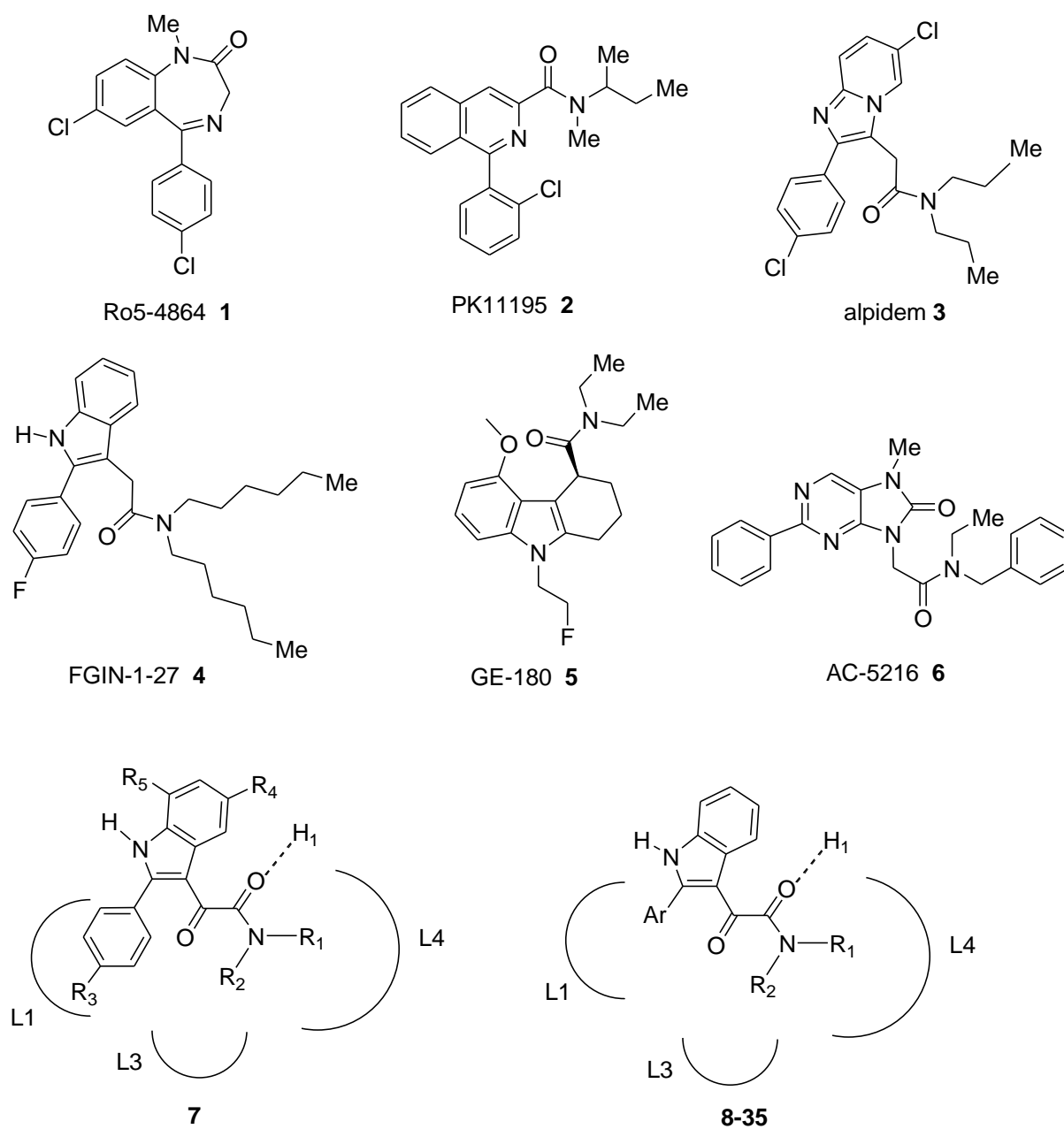


Chart 1. Structures of known (**1-7**) and newly synthesized (**8-35**) TSPO ligands. Structures **7-35** have been drawn embedded within a pharmacophore/topological model of ligand-TSPO interaction.^{25,26,28}

“Table of Contents graphic.”

